Seismic- and well-log-inferred gas hydrate accumulations on Richards Island

T.S. Collett[1], M.W. Lee[1], S.R. Dallimore[2], and W.F. Agena[1]

Collett, T.S., Lee, M.W., Dallimore, S.R, and Agena, W.F., 1999: Seismic- and well-log-inferred gas hydrate accumulations on Richards Island; in *Scientific Results from JAPEX/JNOC/GSC Mallik 2L-38 Gas Hydrate Research Well, Mackenzie Delta, Northwest Territories, Canada, (ed.) S.R. Dallimore, T. Uchida, and T.S. Collett; Geological Survey of Canada, Bulletin 544, p. 357–376.*

Abstract: The gas hydrate stability zone is areally extensive beneath most of the Mackenzie Delta-Beaufort Sea region, with the base of the gas hydrate stability zone more than 1000 m deep on Richards Island. In this study, gas hydrate has been inferred to occur in nine Richards Island exploratory wells on the basis of well-log responses calibrated to the response of the logs within the cored gas-hydrate-bearing intervals of the JAPEX/JNOC/GSC Mallik 2L-38 gas hydrate research well. The integration of the available well-log data with more than 240 km of industry-acquired reflection seismic data have allowed us to map the occurrence of four significant gas hydrate and associated free-gas accumulations in the Ivik–Mallik–Taglu area on Richards Island. The occurrence of gas hydrate on Richards Island is mostly restricted to the crest of large anticlinal features that cut across the base of the gas hydrate stability zone. Combined seismic and well-log data analysis indicate that the known and inferred gas hydrate accumulations on Richards Island may contain as much as 187 178x10^6 m^3 of gas.

Résumé : La zone de stabilité des hydrates de gaz est très étendue sous la quasi totalité de la région du delta du Mackenzie et de la mer de Beaufort; dans l'île Richards, sa base est située au-delà de 1 000 m de profondeur. Dans la présente étude, on a déduit que dans l'île Richards, neuf puits d'exploration contenaient des hydrates de gaz en se basant sur les réponses obtenues de diagraphies de puits étalonnées d'après les réponses des diagraphies effectuées dans les intervalles à hydrates de gaz carottés du puits de recherche sur les hydrates de gaz JAPEX/JNOC/GSC Mallik 2L-38. L'intégration de données diagraphiques disponibles à plus de 240 km de données de sismique-réflexion acquises par le secteur privé nous a permis de cartographier quatre accumulations importantes d'hydrates de gaz et de gaz libre associé dans la région d'Ivik–Mallik–Taglu, dans l'île Richards. Dans cette île, les hydrates de gaz sont pour la plupart confinés dans la crête de grandes structures anticlinales qui recoupent la base de la zone de stabilité des hydrates de gaz. Les analyses regroupées de données sismiques et diagraphiques révèlent que dans l'île Richards, les accumulations d'hydrates de gaz connues et possibles pourraient contenir jusqu'à 187 178 x 10^6 m^3 de gaz.

[1] United States Geological Survey, Denver Federal Center, Box 25046, MS-939, Denver, Colorado 80225, U.S.A.
[2] Geological Survey of Canada, 601 Booth Street, Ottawa, Ontario, Canada K1A 0E8

INTRODUCTION

Even though gas hydrate deposits are known to occur in numerous Arctic sedimentary basins, little is known about the geological parameters controlling their formation and occurrence. The primary objective if this report is to integrate the available geological and geophysical data, including conventional open-hole well-log data from 11 previously drilled industry exploratory wells and over 240 km of industry-acquired reflection seismic data, in order to assess the distribution and size of the gas hydrate and associated free-gas accumulations in the area of the Ivik, Mallik, and Taglu conventional gas fields on Richards Island in the outer Mackenzie Delta (Fig. 1). This report documents the occurrence of four distinct well-log- and seismic-inferred gas hydrate accumulations in the Ivik–Mallik–Taglu area on Richards Island. In addition, the geological controls on the occurrence of these four inferred gas hydrate accumulations have also been evaluated. This evaluation has resulted in the development of a hydrate 'play' model that can be used to explain the occurrence of the Ivik–Mallik–Taglu gas hydrate accumulations and predict where similar occurrences might be found in unexplored regions.

This paper begins with a detailed review of the methodology used to process and interpret the available industry open-hole well-log and seismic reflection data. This paper also includes a review of the geological setting of the Richards Island area of the outer Mackenzie Delta, which is followed by a discussion of the results of the log and seismic data interpretation portion of this study. The paper concludes with a description of the four inferred gas hydrate accumulations in the Ivik–Mallik–Taglu area, including an estimate of the volume of gas within the four delineated gas hydrate accumulations.

METHODOLOGY

Available data

Conventional open-hole well-log data from 11 industry exploratory wells (including the JNOC/JAPEX/GSC Mallik 2L-38 gas hydrate research well) located on Richards Island were obtained to assess the occurrence of gas hydrate and associated free-gas accumulations in the Ivik–Mallik–Taglu area (Fig. 2, Table 1). With the exception of the Mallik 2L-38 well, all of the wells examined in this study were drilled in the early 1970s as industry exploration wells designed to test the

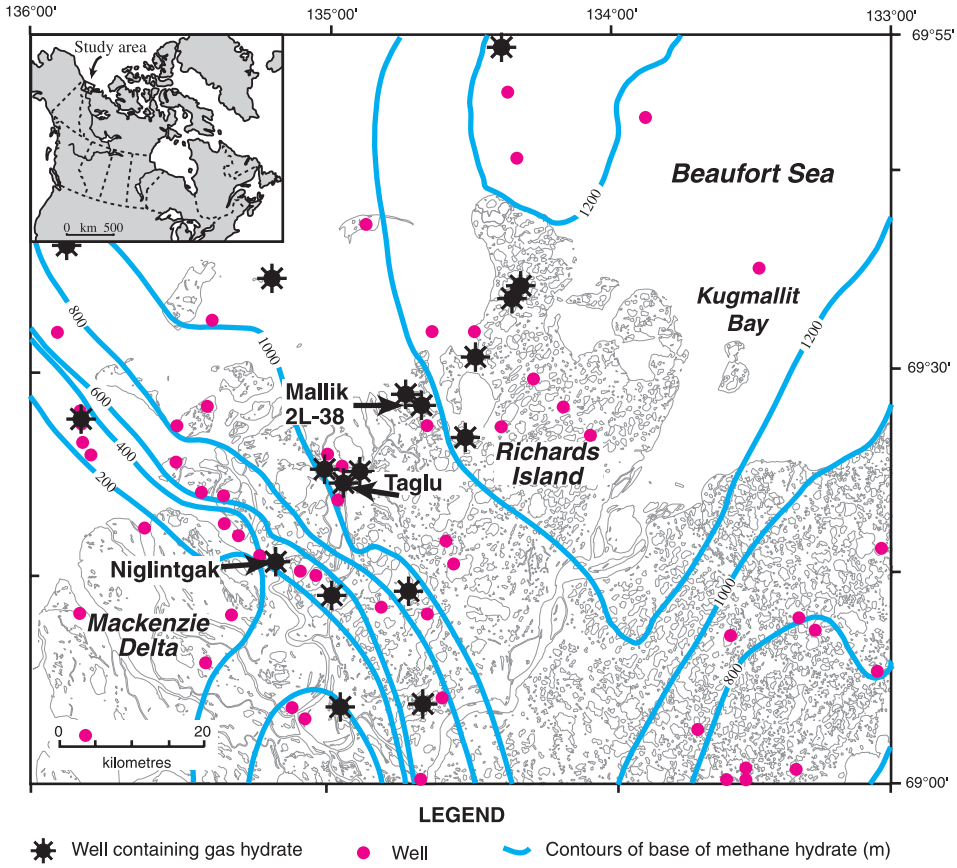

Figure 1. *Map of part of the Mackenzie Delta region showing the calculated depth to the base of the methane hydrate stability zone (Dallimore and Collett, 1999).*

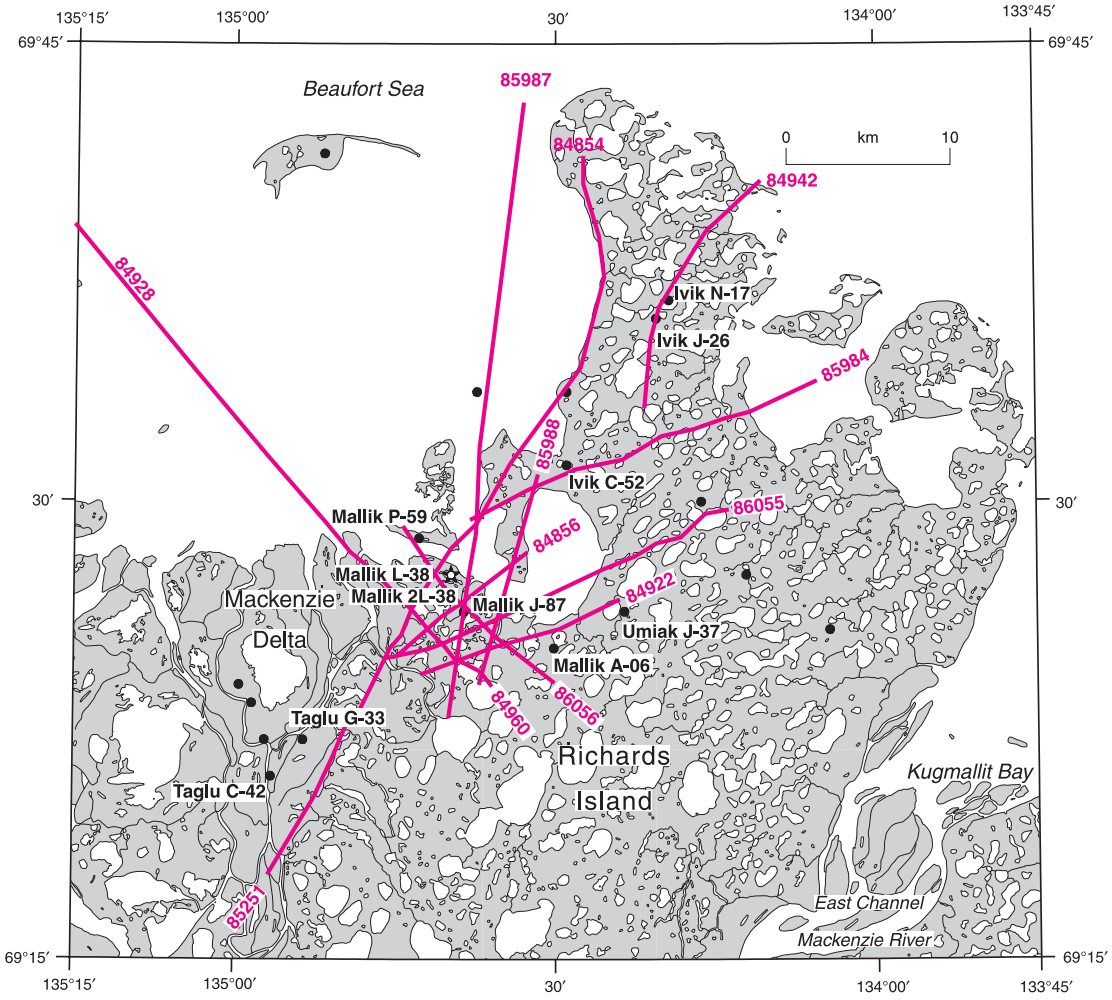

Figure 2. *Map of a portion of Richards Island in the outer Mackenzie Delta showing the location of reflection seismic profiles and wells having downhole wire-line log surveys that were used in this study.*

Table 1. List of wells from Richards Island with downhole wireline log data used in this study. Also listed for each well is the elevation of the drilling-rig kelly bushing, elevation of the ground surface at the well site, estimated depth of the base of permafrost (modified from Majorowicz and Smith, 1999), depth to the base of the predicted methane hydrate stability zone (modified from Majorowicz and Smith, 1999), and the depth of the pertinent sequence boundaries (J. Dixon, pers. comm., 1999).

Well name	Elevation of kelly bushing (m)	Elevation of ground surface (m)	Depth to base of permafrost (m)*	Depth to base of gas hydrate stability zone (m)*	Depth to the Iperk-Mackenzie Bay sequence boundary (m)*	Depth to the Mackenzie Bay-Kugmallit sequence boundary (m)*	Depth to the Kugmallit-Richards sequence boundary (m)*
Ivik J-26	27.4320	20.1168	500	1200*	488	881	2091
Ivik N-17	35.2653	28.2549	672	1300	483	902	2193
Ivik C-52	21.6408	12.8016	649	1300	394	610	1664
Mallik L-38	9.8750	0.8839	613	1100	339	858	1924
Mallik 2L-38	8.4100	1.3600	613	1100*	339	858	1924
Mallik P-59	8.1381	1.0058	645	1200	366	769	1811
Mallik J-37	28.8645	20.4825	622	1300	307	593	1340
Mallik A-06	35.4787	27.3100	640	1300	269	607	1271
Umiak J-37	28.8645	20.4825	669	1300	398	706	1611
Taglu G-33	7.9248	1.8288	543	1100	337	816	1531
Taglu C-42	13.4112	1.524	600	1100	341	567	1616

*Depths measured from ground level

more deeply buried conventional hydrocarbon accumulations in the region. Therefore, the open-hole well-log data from the shallow, potential gas-hydrate-bearing portion of the wells are often of inferior quality due to poor borehole conditions and in many cases certain types of well logs required to completely assess potential gas hydrate occurrences in the near-surface sedimentary section (<1500 m) were never obtained. However, the available open-hole logs from the 11 wells examined in this study were sufficient to evaluate the occurrence of gas hydrate and free gas in the well-log- and seismic-inferred gas hydrate accumulations in the Ivik–Mallik–Taglu area of Richards Island.

Digital files for 13 reflection seismic profiles, totalling about 240 km of data, were obtained from Imperial Oil Limited for a portion of Richards Island within the outer Mackenzie Delta (Fig. 2, Table 2). This seismic data was acquired for conventional oil and gas exploration purposes in 1984 and 1985, so the field parameters were not optimum for the evaluation of shallow gas-hydrate-related features. However, specialized reprocessing provided the information needed to understand the distribution of gas hydrate and associated free-gas accumulations. The reprocessed seismic data also provided valuable insight to the sedimentological and structural features controlling the distribution of the gas hydrate accumulations on Richards Island.

Well-log data evaluation

Within oil and gas exploration wells drilled in the Arctic, the permafrost-bearing and gas-hydrate-bearing intervals are usually drilled and cased before drilling to greater depths. All 11 wells examined in this study were drilled in a similar fashion (Fig. 2, Table 1), however, most of the well-log-inferred gas-hydrate-bearing units in the Ivik–Mallik–Taglu area wells (well-log-inferred gas hydrate occurrences are discussed in more detail later in this report) occur below the depth of the 'permafrost' casing which was usually set either within or above the well-log-inferred gas-hydrate-bearing units. Before logging the subpermafrost gas hydrate accumulations in the Ivik–Mallik–Taglu area wells, the borehole was usually advanced to a depth of at least 3000 m. This subjected the potential gas-hydrate-bearing units within the subpermafrost section of each well (below about 700 m) to significant thermal disturbance, and could cause gas hydrate within the formation near the well bore to disassociate. In several of the wells examined as part of this study, the breakdown of the in situ gas hydrate caused significant borehole stability problems which contributed to the development of large borehole 'washouts' within the subpermafrost gas-hydrate-bearing units. The quality of the log measurements in most of the wells used in this study were moderately to severely degraded by the size and rugosity of the borehole. The log evaluation methods used to identify and quantitatively assess the gas hydrate accumulations in the Ivik–Mallik–Taglu area wells are described in the 'Well-log data interpretation' section of this report, which also contains a detailed review of the logs available from each well examined in this study.

The subsurface depths used for each well in this paper are given in depth below ground surface, which was calculated by subtracting the height above ground surface of the kelly bushing (log depths were measured from the kelly bushing) on the drilling rig from the downhole measured log depths (*see* listing, Table 1).

Table 2. List of seismic profiles from Richards Island used in this study.

Seismic profile name	Year acquired	Length of seismic profile (km)	Nominal fold	Common-mid-point interval (CMP) (m)	Acoustic source
E84854	1984	26.8	20	25	Dynamite
E84856	1984	10.2	15	20	Dynamite
E84867	1984	12.3	15	17	Dynamite
E84922	1984	13.1	15	20	Dynamite
E84928	1984	18.4	15	20	Dynamite
E84942	1984	16.5	20	25	Dynamite
E84960	1984	19.4	16	20	Vibroseis
E85251	1984	26.9	15	20	Dynamite
E85984	1985	20.5	15	25	Dynamite
E85987	1985	27.9	32	20	Dynamite
E85988	1985	13.2	15	25	Dynamite
E86055	1985	24.4	20	25	Dynamite
E86056	1985	13.5	20	25	Dynamite

Seismic data processing

The methods and processing steps used to reprocess the Imperial Oil Limited seismic data from the Ivik–Mallik–Taglu area are displayed in the processing flowchart in Figure 3 and all relevant information pertaining to the available seismic lines is listed in Table 2. All of the seismic data was stacked and migrated using dip-moveout (DMO) corrected velocities. In order to use reflection amplitudes to map the distribution of gas hydrate and free gas, a processing strategy capable of preserving the relative true amplitudes was applied. The important steps in relative true amplitude processing are 1) editing noisy traces, 2) applying programmed gain functions, and 3) compensating for differences in the source strength, receiver coupling, and other surface-related amplitude variations. A programmed gain function, T^2, was applied to the data and a spectral balancing was applied as a deconvolution procedure. In order to compensate for the amplitude variation related to the surface conditions, a process called surface consistent amplitude correction (SCAC) was applied. This process compensates for variations in amplitudes owing to the strength of the shot, the response and coupling of the receivers, and the performance of amplifier channels, all of which are not related to reflection amplitudes in a surface-consistent manner. This process estimates the trace amplitude based on source, offset, common midpoint (CMP) and channel, and it contributes and decomposes each contribution and adjusts the amplitude variation. Poststack wavelet deconvolution and zero-crossing predictive deconvolution were applied to all seismic data in order to increase temporal resolution and to remove the differences of the source wavelets. For a more complete review of the seismic data processing techniques used in this study, including prestack depth migration and migration velocity analysis, see the complete seismic data processing report by Lee and Agena (1998).

As previously noted, the recording parameters for this data were not optimum for mapping shallow gas-hydrate-related features (less than about 1500 m deep). However, careful processing, including spectral whitening before stacking, poststack second zero-crossing predictive deconvolution, and wavelet deconvolution provided adequate seismic sections for interpreting the shallow gas-hydrate-related features in the Ivik–Mallik–Taglu area.

GEOLOGICAL SETTING

Regional geology

The geology of the Mackenzie Delta region has been described in numerous publications (Dixon et al., 1992, 1994). Surficial sediments of the Mackenzie Delta (Fig. 1) are composed in part of modern deltaic sediments and of older fluvial and glacial deposits of Richards Island and the Tuktoyaktuk Peninsula. At depth, this region is underlain by Mesozoic and Cenozoic deltaic sandstone and shale units that thicken to more than 12 km over a short distance seaward from the present shoreline. This sedimentary section overlies faulted Paleozoic rocks stepping down steeply beneath the Mesozoic and Cenozoic section.

The post-Paleozoic sedimentary rocks of the Beaufort Sea continental shelf are subdivided into two major sections, pre-Upper Cretaceous and Upper Cretaceous to Holocene strata. A major regional unconformity marks the boundary between the Upper Cretaceous and older strata (Dixon et al., 1992). Above this regional unconformity, sedimentation was dominated by deltaic processes, resulting in a series of thick, generally northward-prograding delta complexes, to which lithostratigraphic terminology can be applied (Dixon et al., 1992). Within the study area, nine sequences have been identified using reflection seismic records, well data, and outcrop data (Fig. 4). Within the Ivik–Mallik–Taglu area of Richards Island the zone of predicted methane hydrate stability (discussed later in this report) is spatially limited to portions of only four of the delineated sequences: Iperk Sequence, Mackenzie Bay Sequence, Kugmallit Sequence, and Richards Sequence. On Richards Island, the middle Eocene to late Eocene Richards Sequence is predominantly a mudstone

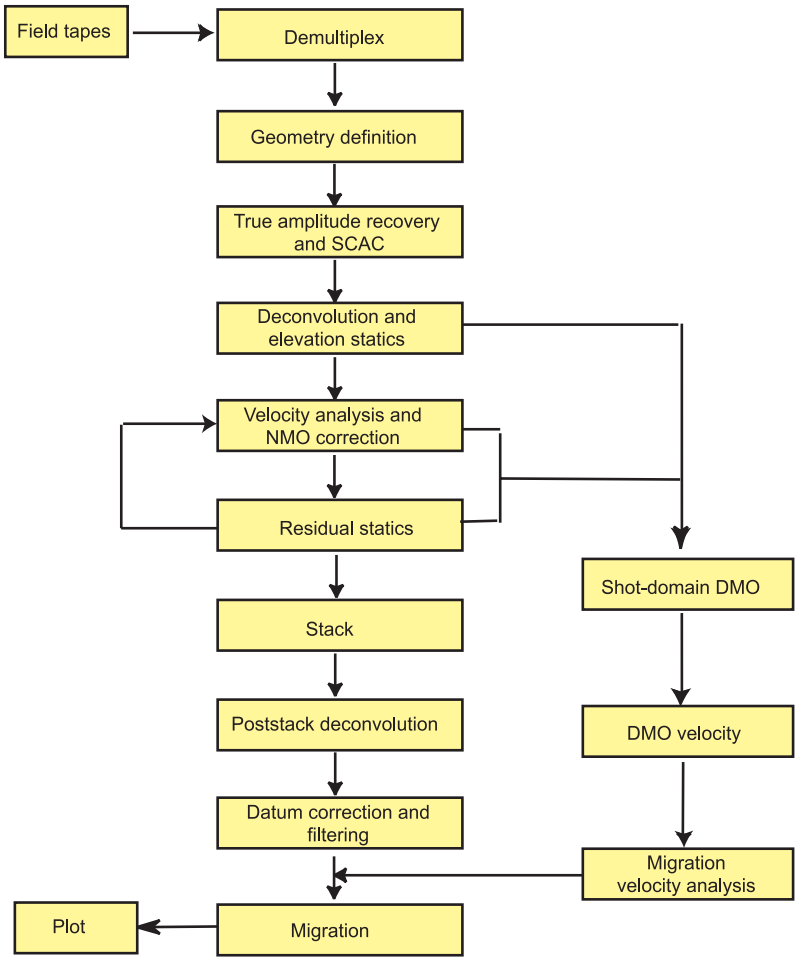

Figure 3.

Seismic data processing flow chart.

SCAS: surface consistent amplitude correction
NMO : normal moveout
DMO: dip moveout

succession of prodelta and slope deposits. Locally, in the Mackenzie Delta area, the Richards Sequence is unconformably overlain by Kugmallit Sequence strata. The Oligocene Kugmallit Sequence consists of sand-dominated delta-plain deposits, sand and mud of delta front origin, and deep-water muds and silts. The Late Oligocene to Middle Miocene Mackenzie Bay Sequence rests abruptly, and locally unconformably, on Kugmallit Sequence and older strata. In the central part of the Mackenzie Delt–Beaufort Sea Basin the Mackenzie Bay Sequence is predominantly a mudstone to siltstone succession. Within the study area, the Mackenzie Bay Sequence is unconformably overlain by the upper Miocene to Pleistocene Iperk Sequence. Along the margin of the basin, the progradational Iperk Sequence consists of nonmarine to marginal marine sand and gravel deposits, which grade laterally into the basin as continental-slope mud and silt deposits.

The Tertiary sedimentary rocks of the Mackenzie Delta region are deformed by large-scale growth faults, particularly along the basin margin. A distinct tectonostratigraphic break occurs between the Late Oligocene to Middle Miocene Mackenzie Bay Sequence and the upper Miocene to Pleistocene Iperk Sequence. Most of the early to mid-Tertiary structural features are truncated at the unconformity surface marking the base of the Iperk Sequence. This late Miocene unconformity marks the end of significant tectonism within the Mackenzie Delta region.

Hydrocarbon occurrences

Since the beginning of significant oil exploration in 1962, over 240 petroleum exploration wells have been drilled in the Mackenzie Delt–Beaufort Sea region. More than 40 hydrocarbon accumulations have been discovered, containing an estimated $238 \times 10^6 m^3$ to $317 \times 10^6 m^3$ (1.5×10^9 to 2.0×10^9 barrels) of recoverable oil and $292 \times 10^9 m^3$ to $356 \times 10^9 m^3$ (10.4×10^{12} ft.^{3} to12.6×10^{12} ft.^{3}) of recoverable gas (Dixon et al., 1994). At least 26 of these oil and gas fields have been discovered in the Tertiary rock sequences of the Mackenzie Delta–Beaufort Sea region (Procter et al., 1984). The Taglu and Niglintgak fields contain most of the cumulative gas reserves in the region (Dixon et al., 1994). These two hydrocarbon accumulations occur within the late Paleocene to early Oligocene Reindeer and Kugmallit sequences, and are stratigraphically below the gas-hydrate-bearing Oligocene to Pleistocene reservoirs (discussed below). The gas within these Tertiary fields was generated in adjacent shale units, which are described as being thermally immature and dominated by land-derived herbaceous organic material (Snowdon and Powell, 1982). The type III terrestrial organic material accounts for the low temperature generation of the large Tertiary gas reserves. In the offshore part of the Mackenzie

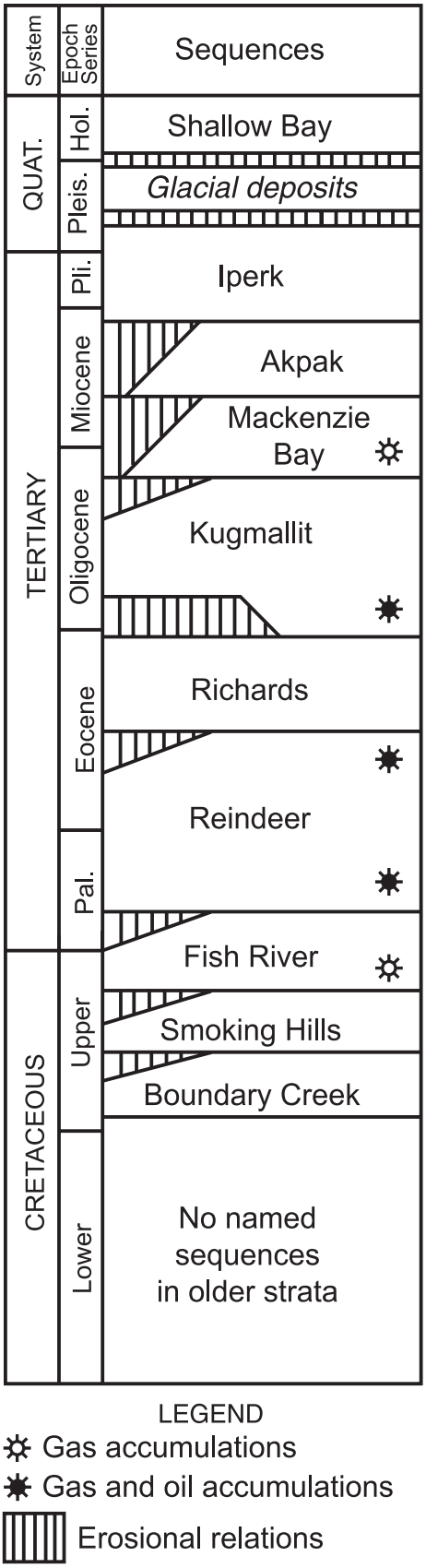

Figure 4. *Stratigraphic column for the Mackenzie Delta region, Northwest Territories, Canada. Sequence terminology modified from Dixon et al. (1992). Well symbols indicate stratigraphic location of hydrocarbon production. Quat.=Quaternary, Pal.=Paleocene, Pli.=Pliocene, Pleis.=Pleistocene, Hol.=Holocene.*

Delta region, beyond the 20 m bathymetric contour, oil and gas have been derived from a mixture of terrestrial and marine organic matter, which is evidence of extensive migration from more mature, deeply buried sources (Snowdon and Powell, 1982).

Permafrost

Temperature data from industry boreholes in the Mackenzie Delta region reveal that the thermal regime within 1 km of the surface is highly complex due to widely varying surface-temperature histories and significant variations in subsurface lithologies (Allen et al., 1988). In the Mackenzie Delta region, ice-bearing permafrost, as interpreted from industry geophysical well logs, reaches a maximum thickness of about 700 m on Richards Island and generally thins offshore (Judge, 1986). Ice-bearing permafrost beneath the modern Mackenzie Delta is thin to absent, and no ice-bearing sediments have been observed in offshore areas where water depths exceed 80 m (Allen et al., 1988). In the area of the Ivik, Mallik, and Taglu conventional gas fields on Richards Island the base of ice-bearing permafrost extends to more than 600 m deep (Fig. 5). Whereas to the southwest, towards the central portion of the modern Mackenzie Delta, the base of ice-bearing permafrost is less than 100 m below the surface (Judge, 1986).

Gas hydrate

Natural gas hydrate deposits are thought to occur in 25 Mackenzie Delta–Beaufort Sea exploratory wells (Smith and Judge, 1993). All of these inferred gas hydrate deposits occur in clastic sedimentary rocks of the Tertiary Kugmallit, Mackenzie Bay, and Iperk sequences (Procter et al., 1984; Dixon et al., 1992, 1994; Smith and Judge, 1993). Gas hydrate was also recovered in a core at a depth of 336.4 m in the 92GSCTAGLU borehole (Dallimore and Collett, 1995). The occurrence of gas hydrate is limited to a certain range of temperature and pressure conditions (Sloan, 1990); therefore, the physical limits of the zone in which conditions are suitable for gas hydrate formation can be determined. Maps of the methane-gas hydrate stability zone in the Mackenzie

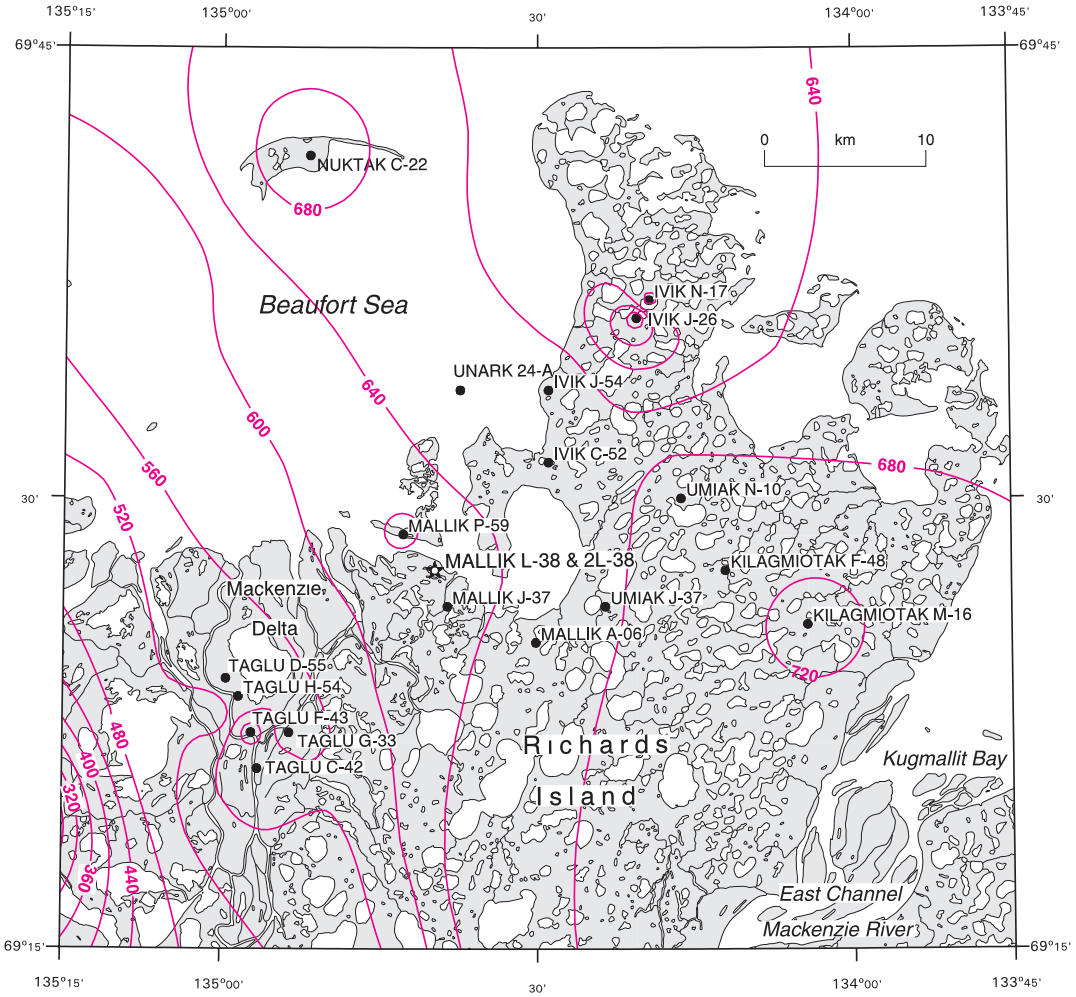

Figure 5. *Map showing the depth to the base of permafrost for a portion of Richards Island in the outer Mackenzie Delta (Majorowicz and Smith, 1999).*

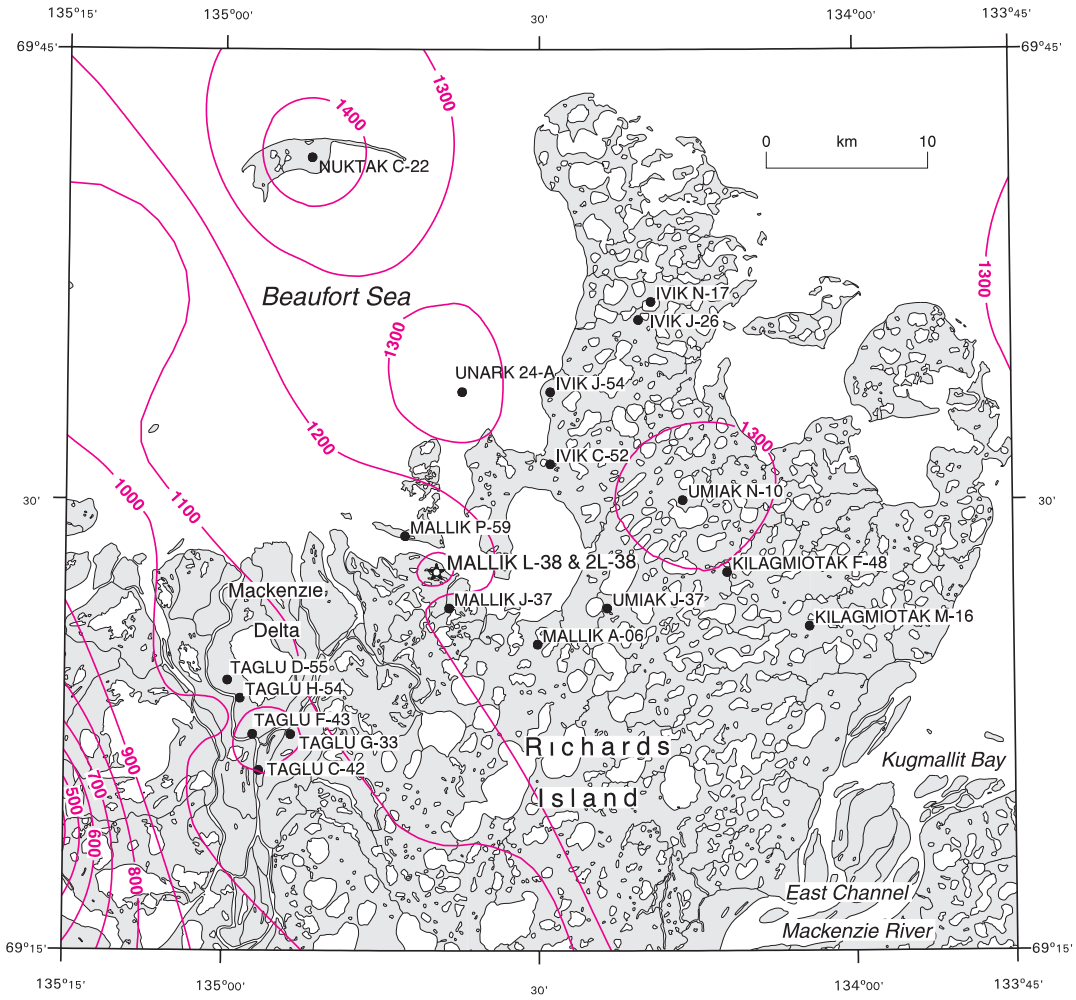

Figure 6. *Map showing the depth to the base of the 'predicted' methane-gas hydrate stability zone for a portion of Richards Island in the outer Mackenzie Delta (Majorowicz and Smith, 1999). It should be noted that contours were constructed using weighted moving average technique and as a result contour lines may vary somewhat from Table 1.*

Delta–Beaufort Sea sedimentary basin (Fig. 6) show that the zone in which methane hydrate can occur extends to depths greater than 1200 m on Richards Island and is extensive beneath most of the continental shelf area (Judge and Majorowicz, 1992).

Prior to the recently completed JNOC/JAPEX/GSC Mallik 2L-38 gas hydrate research well, the most extensively studied gas hydrate occurrences on Richards Island were those drilled in the Mallik L-38 and Ivik J-26 wells (Bily and Dick, 1974). It is estimated that the Mallik L-38 and Mallik 2L-38 wells encountered more than 100 m of gas-hydrate-bearing sediments (Dallimore and Collett, 1999; Collett et al., 1999), and the Ivik J-26 well penetrated about 25 m of gas hydrate (Bily and Dick, 1974). The well-log-inferred gas-hydrate-bearing sediments in the Mallik L-38 and Mallik 2L-38 wells occur within the predicted methane hydrate stability zone and below the base of ice-bearing permafrost. The gas hydrate occurrences in the Ivik J-26 well are very similar to those in the Mallik L-38 and also occur within the predicted methane hydrate stability zone and below the base of ice-bearing permafrost. All of the well-log-inferred gas hydrate in the Mallik and Ivik area occur in clastic sedimentary rocks of the Kugmallit and Mackenzie Bay sequences.

WELL-LOG DATA INTERPRETATION

Well-log evaluation of in situ gas hydrate and free gas

In most gas hydrate studies only two well-logging devices are consistently used to identify potential gas hydrate; they are the electrical resistivity and acoustic transit-time logs. In comparison to water-saturated sediments, gas-hydrate-bearing sediments exhibit anomalously high electrical resistivities and rapid acoustic transit-times (high acoustic velocities). However, electrical resistivity and acoustic logs behave similarly within sedimentary units saturated with either gas

hydrate or ice. Hence, the indication of gas shows (produced from decomposing gas hydrate) on the mud log often provides the only means of conclusively differentiating a gas hydrate from ice. However, the focus of this study is gas hydrate accumulations occurring below the base of ice-bearing permafrost.

The velocity of a compressional acoustic wave in a solid medium, such as gas-hydrate-bearing sediment, is usually several times greater than the velocity of a compressional acoustic wave in a gas-bearing sediment. In most well-log studies, gas-bearing zones highly attenuate compressional acoustic waves and appear as anomalous low-velocity zones. Therefore, at the base of the gas hydrate stability zone, which marks the contact between gas-hydrate- and free-gas-bearing sediments, the acoustic log is often characterized by a distinct drop in acoustic velocity from the gas-hydrate-bearing section above into the underlying free-gas-bearing interval.

In the following section of this report, we have used the available downhole log data from the Ivik–Mallik–Taglu wells to identify potential in situ gas hydrate occurrences and to calculate sediment porosities and gas hydrate saturations within the well-log-inferred gas-hydrate-bearing stratigraphic units. However, before proceeding with the examination of the log data from the Ivik–Mallik–Taglu wells it is necessary to review the well-log evaluation techniques we used to calculate sediment porosities and gas hydrate saturations.

When available, the unedited bulk-density (ρ_b) log measurements were used to calculate sediment porosities (ϕ) in the wells examined using the standard density-porosity relation of Collett (1998b):

$$\phi = \frac{\rho_m - \rho_b}{\rho_m - \rho_f} \quad (1)$$

Within this equation, the density of the formation waters (ρ_f) was assumed to be constant and equal to 1.00 g/cm^3 and the grain/matrix densities (ρ_m) were assumed to equal 2.65 g/cm^3.

In the following section of this report, the Archie relation (Archie, 1942) has been used to calculate water saturations (S_w) (gas hydrate saturation (Sh) is equal to (1.0-S_w)) from the available electrical resistivity log data in some of the wells from the Ivik–Mallik–Taglu area. The resistivity approach used to assess gas hydrate saturations in this study was based on the 'standard' Archie equation:

$$S_w = \left(\frac{aR_w}{\phi^m R_t} \right)^{\frac{1}{n}} \quad (2)$$

(Collett, 1998a). As discussed above, the porosity data needed for the Archie equation were derived from the available downhole density logs and the standard density-porosity relation (Collett, 1998b). In addition to porosity, the Archie relation also requires as input the value of the empirical Archie constants (*a, m,* and *n*), the resistivity of the in situ pore waters (R_w), and the resistivity of the formation (R_t) which is obtained from the deep resistivity logs in each well.

We have used the so-called 'Humble' values for the *a* (0.62) and *m* (2.15) Archie constants which are considered applicable for granular matrix systems (Collett, 1998a). The value of the empirical constant *n* was assumed to be 1.9386 as determined by Pearson et al. (1983). The resistivity of pore waters (R_w) is mainly a function of the temperature and the dissolved salt content of the pore waters. It has been determined that the average pore-water salinity of the formation waters in the Mackenzie Delta–Beaufort Sea region, within the depth range from 200 m to 2000 m, is approximately 10 parts per thousand (ppt) (Collett and Dallimore, 1998). However, pore-water salinity data from the analysis of interstitial water samples collected from formation production tests in the gas-hydrate-bearing section of the Mallik L-38 and Ivik J-26 wells yielded anomalously high values ranging from 20 parts per thousand (ppt) to near 30 ppt, and averaged about 25 ppt. In addition, the analyses of pore-water samples from the recovered cores in the Mallik 2L-38 well also appear to be enriched in salt, with pore-water salinities ranging near 1–2 ppt in the gas-hydrate-bearing cores to over 35 ppt in the water-saturated portions of the cores (Cranston, 1999). It is possible that solute exclusion during gas hydrate formation has locally enriched the dissolved salt content of the pore waters that occur in close proximity to gas hydrate accumulations in the Ivik–Mallik–Taglu area. Therefore, the higher pore-water salinities, averaging near 25 ppt, calculated from the production test water samples likely represents the in situ salinity of the pore waters in the Ivik–Mallik–Taglu area. Formation temperature data in the Ivik–Mallik–Taglu area wells are available from downhole temperature surveys, yielding subpermafrost geothermal gradients ranging from 2.4°C/100 m to 3.6°C/100 m and base of permafrost depths ranging from 500 m to 672 m (Table 1). In each well examined, Arps' formula (Collett, 1998a) was used to calculate the pore-water resistivities (R_w) from the assumed interstitial water salinity of 25 ppt and the measured formation temperatures. Given the Archie constants (*a*, *m,* and *n*) and pore-water resistivities (R_w), it was then possible to calculate water saturations (S_w) (gas hydrate saturation (Sh) is equal to (1.0-S_w)) within the Ivik–Mallik–Taglu area wells.

It is important to note that the average sediment porosities and water saturations (S_w) (gas hydrate saturation (Sh) is equal to (1.0-S_w)) reported is this paper have been calculated by averaging the porosity and saturation values for the entire 'gas hydrate interval' which in most cases includes both gas-hydrate- and non-gas-hydrate-bearing sedimentary sections. Therefore, the methods used to calculate average sediment porosities and water saturations in this paper are internally consistent. However, the average sediment porosity and water saturation values reported in this paper may differ from values reported in other papers from this volume.

Well-log data interpretation — results

Ivik J-26 well

The Ivik J-26 well was drilled to a depth of 3639 m by Imperial Oil Limited in April of 1972. The base of ice-bearing permafrost in the Ivik J-26 well, as interpreted from available electrical resistivity and acoustic transit-time logs, is estimated at 500 m (Table 1). The base of the methane hydrate stability

zone as predicted from borehole temperature surveys is at a depth of 1200 m (Table 1). The subpermafrost section of the Ivik J-26 well was surveyed with dual-induction-laterolog (DIL), gamma-ray (GR), borehole-compensated acoustic transit-time (BHC), and compensated formation density (FDC) well-logging devices.

As previously discussed, Bily and Dick (1974) determined that the Ivik J-26 well penetrated about 25 m of gas-hydrate-bearing sediments within the depth interval from 973.9 m to 1014.1 m. The well-log-inferred gas-hydrate-bearing sediments in the Ivik J-26 well exhibit very high acoustic velocities and electrical resistivities on the recorded downhole logs which are indicative of gas-hydrate-bearing sediments. The analysis of downhole-log-measured acoustic transit-time velocities and electrical resistivities in the Ivik J-26 well revealed no evidence of in situ free gas below the well-log-inferred gas hydrate occurrence.

The density-log porosities in the gas-hydrate-bearing units of the Ivik J-26 well, calculated using the standard density-porosity relation, average 36% (Table 3). The water saturations (S_w) calculated with the Archie relation within the interval from 973.9 m to 1014.1 m in the Ivik J-26 well averaged 50% (Table 3).

Ivik N-17 well

The Ivik N-17 well was also drilled by Imperial Oil Limited in 1973 to a depth of 3040 m. The base of ice-bearing permafrost in the Ivik N-17 well is estimated at 672 m and the base of the methane hydrate stability zone, as predicted from borehole temperature surveys, is at a depth of 1300 m (Table 1). The subpermafrost section of the Ivik N-17 well was surveyed with dual-induction-laterolog (DIL), gamma-ray (GR), borehole-compensated acoustic transit-time (BHC), and compensated formation density (FDC) well-logging devices.

The analysis of acoustic transit-time and electrical resistivity logs from the Ivik N-17 well reveals no conclusive evidence of in situ gas hydrate. However, the subsequent analysis of water saturations from the available electrical-resistivity and density-porosity data reveals a relatively thick gas hydrate occurrence in the Ivik N-17 well within the depth interval from 960.6 m to 1057.8 m, which is near the same depth of the gas hydrate occurrence in the Ivik J-26 well. Analysis of downhole well logs from the Ivik N-17 well revealed no evidence of in situ free gas below the well-log-inferred gas hydrate occurrence.

The density-log-calculated porosities in the well-log-inferred gas-hydrate-bearing units in the Ivik N-17 well average 37% (Table 3). The water saturations (S_w) (gas hydrate saturation (Sh) is equal to (1.0-S_w)) calculated with the Archie relation within the gas-hydrate-bearing interval of the Ivik N-17 well are relatively high, averaging 91% (Table 3).

Ivik C-52 well

The Ivik C-52 well was drilled by Imperial Oil Limited in late 1972 to a depth of 3037 m. The base of ice-bearing permafrost in the Ivik C-52 well as interpreted from available electrical resistivity and acoustic transit-time logs is estimated at 649 m (Table 1). The base of the methane hydrate stability zone as predicted from borehole temperature surveys is at a depth of 1300 m (Table 1). The subpermafrost section of the Ivik C-52 well was surveyed with only the dual-induction-laterolog (DIL), gamma-ray (GR), and borehole-compensated acoustic transit-time (BHC) well-logging devices. None of the predicted methane hydrate stability zone was logged with a density-logging device, thus limiting our assessment of this well.

Based on the analysis of the downhole-recorded electrical resistivities and acoustic velocities, it appears that the Ivik C-52 well penetrated a relatively thick gas-hydrate-bearing

Table 3. List of wells from Richards Island inferred to have penetrated gas hydrate based on well-log responses. Also listed for each well is the depth to the top and bottom of the well-log-inferred gas hydrate occurrences, the depth of the well-log-inferred base of gas hydrate stability (gas hydrate–free-gas contact), total thickness of the well-log-inferred gas-hydrate-bearing interval in each well, density-log-derived sediment porosity of the well-log-inferred gas hydrate occurrence in each well, well-log-derived water saturations of the well-log-inferred gas hydrate occurrence in each well, and the 'per-well hydrate gas yield' factor calculated for each well.

Well name	Depth to the top of the well-log-inferred gas hydrate interval (m)*	Depth to the bottom of the well-log-inferred gas hydrate interval (m)*	Depth to the base of the well-log-inferred gas hydrate stability zone (m)*	Thickness of the well-log-inferred gas hydrate interval (m)*	Sediment porosity (%)	Water saturation (%)	Volume of gas within hydrate per square km (x10^6 m^3)
Ivik J-26	973.9	1014.1	-	40.2	36	50	1187
Ivik N-17	960.6	1057.8	-	97.2	37	91	531
Ivik C-52	793.8	923.8	-	130.0	36	88	921
Mallik L-38	810.1	1102.3	1102.3	292.2	31	67	4902
Mallik 2L-38	888.8	1101.9	1101.9	213.1	31	56	4767
Mallik P-59	840.1	996.9	996.9	156.8	37	85	1427
Mallik A-06	965.4	1148.2	1148.2	182.8	36	86	1511
Taglu G-33	925.7	944.7	-	19.0	37	95	58
Taglu C-42	770.1	1085.1	-	315.0	34	98	351

*Depth measured from ground level

sedimentary section within the depth interval from 793.8 m to 923.8 m, however, there is no evidence of free gas below the log-inferred gas hydrate accumulation in the Ivik C-52 well.

Considering the problem presented by the lack of density-log-derived sediment porosities for this well, the analysis of the Ivik C-52 well deviated from our standard procedure. We have used the available density-porosity log data from the Mallik L-38 and Mallik 2L-38 wells to generate a sediment porosity curve for the subpermafrost portion of the Ivik C-52 well. The sediment porosity curve for the Ivik C-52 well was constructed by statistically projecting a linear trendline through the log-calculated density porosities in the 'reservoir quality' sandstone units in the Mallik L-38 and 2L-38 wells. The 'projected' porosities for the gas-hydrate-bearing stratigraphic interval in the Ivik C-52 well, extrapolated from the porosity log data in the Mallik wells, average 36% (Table 3). The water saturations (S_w) (gas hydrate saturation (Sh) is equal to (1.0-S_w)) calculated with the Archie relation within the gas-hydrate-bearing interval of the Ivik C-52 well average 88% (Table 3).

Mallik L-38 well

The Mallik L-38 well was drilled by Imperial Oil Limited in 1972 to a depth of 2524 m. The base of ice-bearing permafrost in the Mallik L-38 well is estimated at 613 m and the base of the methane hydrate stability zone, predicted from borehole temperature surveys, is at a depth of 1100 m (Table 1). The subpermafrost section of the Mallik L-38 well was surveyed with dual-induction-laterolog (DIL), gamma-ray (GR), and borehole-compensated acoustic transit-time (BHC) well-logging devices. But only a portion of the predicted methane hydrate stability zone was logged with compensated formation density (FDC) and sidewall neutron porosity (SNP) logging devices, thus limiting our quantitative analysis of the Mallik L-38 well.

As previously discussed, the Mallik L-38 well is believed to have penetrated about 110 m of gas-hydrate-bearing sandstone units within the depth interval from 810.1 m to 1102.3 m (Fig. 3 *in* Dallimore and Collett, 1999). The well-log-inferred gas-hydrate-bearing sediments in the Mallik L-38 well exhibited very high acoustic velocities and electrical resistivities on the recorded downhole logs. In addition, low reservoir pressures and slow pressure responses during production test (production test-2: 915–918 m) of the well-log-inferred gas-hydrate-bearing units were also interpreted to indicate the presence of gas hydrate in the Mallik L-38 well (Bily and Dick, 1974).

Bily and Dick (1974) originally interpreted the presence of free gas in contact with gas hydrate in several intervals of the Mallik L-38 well. However, the analyses of log data from the Mallik 2L-38 well confirmed the occurrence of only one relatively thin free-gas zone (1100.5–1101.9 m) at the base of the deepest downhole-log-inferred gas hydrate occurrence at the Mallik drill site (Collett et al., 1999).

The density log porosities in the gas-hydrate-bearing units of the Mallik L-38 well, calculated using the standard density-porosity relation, average 31% (Table 3). The water saturations (S_w) calculated with the Archie relation within the gas-hydrate-bearing interval from 810.1 m to 1102.3 m in the Mallik L-38 well average 67% (Table 3).

Mallik 2L-38 well

The Mallik 2L-38 gas hydrate research well was drilled by JNOC, JAPEX, and the GSC in early 1998 to a depth of 1150 m. Similar to the Mallik L-38 well, the base of ice-bearing permafrost in Mallik 2L-38 is estimated at 613 m and the base of the methane hydrate stability zone, predicted from borehole temperature surveys, is at a depth of 1100 m (Table 1). The subpermafrost section of the Mallik 2L-38 well was surveyed with the Schlumberger Platform Express (HALS-PLATFORM-ARI), Array Induction (AIT-EMS-GR-SP), Dipole Shear Sonic Imager (DSI-GR-AMS), and Formation MicroImager (FMI-HNGS) well-logging arrays. The quality of the well logs in the gas-hydrate-bearing portion of the Mallik 2L-38 well is excellent with a near-gauge hole throughout the gas hydrate interval.

Downhole electrical resistivity and acoustic transit-time (both compressional wave and shear wave) logs from the Mallik 2L-38 well confirm the occurrence of in situ gas hydrate at the Mallik drill site within the subsurface depth interval between 888.84 m and 1101.9 m (Fig. 7, in pocket). The cored and logged gas hydrate occurrences in the Mallik 2L-38 well exhibit deep electrical resistivity measurements (ARI) ranging from 10 ohm•m to 100 ohm•m and compressional-wave acoustic velocities (Vp) ranging from 2.5 km/s to 3.6 km/s. In addition, the measured shear-wave acoustic velocities (Vs) of the confirmed gas-hydrate-bearing horizons in the Mallik 2L-38 well range from 1.1 km/s to 2.0 km/s. As noted above, downhole-measured compressional-wave–shear-wave velocity ratios (Vp/Vs) have confirmed the occurrence of a relatively thin free-gas zone (1100.5–1101.9 m) at the base of the deepest downhole-log-inferred gas hydrate in the Mallik 2L-38 well.

The downhole-log-measured bulk densities in the subpermafrost part of the Mallik 2L-38 well are variable with depth (Fig. 7). The density log from Mallik 2L-38 is characterized by numerous thin, low-density zones, ranging in thickness from 2 m to 4 m. Sedimentary and physical property analyses of the recovered cores from the Mallik 2L-38 well confirm that these low-density zones, with measured bulk densities of 1.9 g/cm^3 and lower, contain organic-rich "coals" (Jenner et al., 1999). The density-log porosities in the gas-hydrate-bearing units of the Mallik 2L-38 well calculated using the standard density-porosity relation average 31% (Table 3). The water saturations (S_w) calculated with the Archie relation within the gas-hydrate-bearing interval of the Mallik 2L-38 well average 56% (Table 3).

Mallik P-59 well

The Mallik P-59 well was drilled by Imperial Oil Limited in 1973 to a depth of 2623 m. The base of ice-bearing permafrost in the Mallik P-59 well is estimated at 645 m and the base of the methane hydrate stability zone is predicted from borehole temperature surveys at a depth of 1200 m (Table 1). The

subpermafrost section of Mallik P-59 well was surveyed with only the dual-induction-laterolog (DIL), gamma-ray (GR), and borehole-compensated acoustic transit-time (BHC) well-logging devices. None of the predicted methane hydrate stability zone was logged with a density-logging device, thus limiting our assessment of this well.

The acoustic velocity log in the Mallik P-59 well is characterized by a distinct baseline shift to relatively higher values within the interval from about 840.1 m to 996.9 m. The electrical resistivity log also reveals a small increase of about 1–2 ohm•m within the anomalous high acoustic velocity zone in the Mallik P-59 well. At the base of the anomalously high acoustic velocity zone (depth of 996.9 m), the acoustic velocity log in the Mallik P-59 is marked by an abrupt drop in recorded velocities. An anomalously low velocity interval is seen from 996.9 m to a depth of about 1090 m; velocities within this anomalous interval decrease to 1.5 km/s which suggests the presence of free gas. Based on the analyses of the downhole-recorded electrical resistivities and acoustic velocities, it appears that the Mallik P-59 well penetrated a relatively thick gas-hydrate-bearing sedimentary section within the depth interval from about 840.1 m to 996.9 m, and the distinct drop in acoustic velocity at a depth of 996.9 m marks the contact between gas-hydrate-bearing and free-gas-bearing sediments. In comparison, the base of the methane hydrate stability zone as predicted from borehole temperature surveys (Table 1) is about 200 m deeper than the well-log-inferred gas hydrate–free-gas contact in the Mallik P-59 well. Similar discrepancies have been noted in other gas hydrate studies (Dallimore and Collett, 1998), and have been attributed to either an incomplete subsurface temperature database or unevaluated porous media effect that could shift the theoretical pressure-temperature relationships determined for pure water and methane mixtures.

Considering the problem presented by the lack of sediment porosity data from this well, our log analysis of the Mallik P-59 well deviated from our standard procedure. We have used the available density-porosity log data from the Mallik L-38 and Mallik 2L-38 wells to generate a sediment porosity curve for the Mallik P-59 well. The 'projected' porosities for the gas-hydrate-bearing stratigraphic interval in the Mallik P-59 well average 37% (Table 3). The water saturations (S_w) (gas hydrate saturation (Sh) is equal to (1.0-S_w)) calculated with the Archie relation within the gas-hydrate-bearing interval (840.1–996.9 m) of the Mallik P-59 well average 85% (Table 3).

Mallik J-37 well

The Mallik J-37 well was also drilled by Imperial Oil Limited and was completed to a depth of 3601 m in December of 1972. The base of ice-bearing permafrost in the Mallik J-37 well is estimated at 622 m and the base of the methane hydrate stability zone, predicted from borehole temperature surveys, is at a depth of 1300 m (Table 1). The subpermafrost section of the Mallik J-37 well was logged with a dual-induction-laterolog (DIL), gamma-ray (GR), and borehole-compensated acoustic transit-time (BHC) well-logging devices. However, the zone of predicted methane hydrate stability was not logged with a density device, thus limiting the quantitative analysis of this well.

Similar to the downhole log responses in Mallik P-59, the acoustic velocity log in the Mallik J-37 well is characterized by a baseline shift to relatively higher values within the interval from about 800 m to 1100 m. In comparison to the log responses in Mallik P-59, the electrical resistivity log does not reveal a similar increase in Mallik J-37 and the acoustic well-log response with the inferred gas-hydrate-bearing interval is not as consistent. In addition, at the base of the anomalous high acoustic velocity zone (depth of 1100 m), the acoustic velocity log in the Mallik J-37 well is marked by only a small drop in recorded velocities. Based on the analysis of the downhole-measured acoustic velocities only, it appears that the Mallik J-37 well may have penetrated a relatively thick gas-hydrate-bearing sedimentary section within the depth interval from about 800 m to 1100 m, and the well-log-inferred gas hydrate may be underlain by free gas, however the well-log evidence is inconclusive.

Because of the lack of sediment porosity data and the inconclusive nature of the well-log interpretation of gas hydrate in this well we have not conducted a detailed quantitative analysis of the well-log-inferred gas hydrate in the Mallik J-37 well.

Mallik A-06 well

The Mallik A-06 well was also drilled by Imperial Oil Limited in 1972 to a depth of 4120 m. The base of ice-bearing permafrost in the Mallik A-06 well is estimated at 640 m and the base of the methane hydrate stability zone, predicted from borehole temperature surveys, is at a depth of 1300 m (Table 1). The subpermafrost section of Mallik A-06 well was surveyed with only the dual-induction-laterolog (DIL), gamma-ray (GR), and borehole-compensated acoustic transit-time (BHC) well-logging devices. None of the predicted methane hydrate stability zone was logged with a density logging device, thus limiting our assessment of this well.

The Mallik A-06 well may have penetrated two distinct gas-hydrate-bearing sandstone units within the depth interval from 965.4 m to 1148.2 m. The well-log-inferred gas-hydrate-bearing sediments in the Mallik A-06 well exhibit relatively high acoustic velocities and electrical resistivities on the recorded downhole logs which is indicative of gas-hydrate-bearing sediments. At the base of the deepest log-inferred gas-hydrate-bearing unit (1148.2 m) in the Mallik A-06 well, the acoustic velocity log is marked by an abrupt drop in recorded velocities. However, across this same boundary the electrical resistivity device records a distinct increase in resistivity. An anomalous low-velocity interval is seen from 1148.2 m to a depth of about 1200 m, which suggests the presence of free gas. The increase in electrical resistivities in this interval can also be indicative of free gas. Based on the analysis of the downhole-recorded electrical resistivities and acoustic velocities, it appears that the Mallik P-59 well penetrated several relatively thick gas-hydrate-bearing sedimentary sections within the depth interval from

about 965.4 m to 1148.2 m, and the distinct drop in acoustic velocity at a depth of about 1148.2 m marks the contact between gas-hydrate-bearing and free-gas-bearing sediments. In comparison, the base of the methane hydrate stability zone as predicted from borehole temperature surveys (Table 1) is about 150 m deeper than the well-log-inferred gas hydrate–free-gas contact in the Mallik A-06 well, which again may be attributed to either an incomplete subsurface temperature database or unevaluated porous media effect.

Considering the problem presented by the lack of sediment porosity data from this well, our log analysis of the Mallik A-06 well deviated from our standard procedure. We have used the available density-porosity log data from the Mallik L-38 and Mallik 2L-38 wells to generate a sediment porosity curve for the Mallik A-06 well. The 'projected' porosities for the gas-hydrate-bearing stratigraphic interval in the Mallik A-06 well averages 36% (Table 3). The water saturations (S_w) (gas hydrate saturation (Sh) is equal to (1.0-S_w)) calculated with the Archie relation within the gas-hydrate-bearing interval (965.4–1148.2 m) of the Mallik A-06 well are relatively high, averaging 86% (Table 3).

Umiak J-37 well

The Umiak J-37 well was also drilled by Imperial Oil Limited and was completed to a depth of 3621 m in December of 1972. The base of ice-bearing permafrost in the Umiak J-37 well is estimated at 669 m and the base of the methane hydrate stability zone, predicted from borehole temperature surveys, is at a depth of 1300 m (Table 1). The subpermafrost section of Umiak J-37 well was surveyed with only the dual-induction-laterolog (DIL), gamma-ray (GR), and borehole-compensated acoustic transit-time (BHC) well-logging devices. None of the predicted methane hydrate stability zone was logged with a density logging device, thus limiting our assessment of this well.

The analysis of downhole recorded acoustic velocities and electrical resistivities in the Umiak J-37 wells reveals no evidence of in situ gas hydrate.

Taglu G-33 well

The Taglu G-33 well was drilled by Imperial Oil Limited in 1971 to a depth of 2985 m. The base of ice-bearing permafrost in the Taglu G-33 well is estimated at 543 m and the base of the methane hydrate stability zone, predicted from borehole temperature surveys, is at a depth of 1100 m (Table 1). Only the lower 200 m (900–1100 m) of the predicted methane hydrate stability zone in the Taglu G-33 well was logged with the dual-induction-laterolog (DIL), gamma-ray (GR), borehole-compensated acoustic transit-time (BHC), and compensated formation density (FDC) well-logging devices, thus limiting our assessment of this well.

Based on the analysis of the downhole recorded electrical resistivities and acoustic velocities (below 900 m), it appears that the Taglu G-33 well penetrated three thin (thicknesses ranging from 2 m to 5 m) gas-hydrate-bearing sedimentary units within the depth interval from 925.7 m to 944.7 m. Porosities calculated from the density log for the log-inferred gas-hydrate-bearing units in the Taglu G-33 well average 37% (Table 3). The water saturations (S_w) (gas hydrate saturation (Sh) is equal to (1.0-S_w)) calculated with the Archie relation within the gas-hydrate-bearing interval of the Taglu G-33 well are very high, averaging 95% (Table 3).

Taglu C-42 well

The Taglu C-42 well was also drilled by Imperial Oil Limited and was completed to a depth of 4873 m in May of 1972. The base of ice-bearing permafrost in the Taglu C-42 well is estimated at 600 m and the base of the methane hydrate stability zone, predicted from borehole temperature surveys, is at a depth of 1100 m (Table 1). The subpermafrost section of Taglu C-42 well was surveyed with only the dual-induction-laterolog (DIL), gamma-ray (GR), and borehole-compensated acoustic transit-time (BHC) well-logging devices. None of the predicted methane hydrate stability zone was logged with compensated formation density (FDC) logging device.

Downhole electrical resistivity and acoustic transit-time logs from the Taglu C-42 well infer the occurrence of about 12 gas-hydrate-bearing stratigraphic units within the subsurface depth interval between 770.1 m and 1085 m, with thicknesses of the individual gas-hydrate-bearing units ranging from 2 m to 25 m. Considering the problem presented by the lack of sediment porosity data from this well, our log analysis of the Taglu C-42 well deviated from our standard procedure. We have used the available density-porosity log data from the Mallik L-38, Mallik 2L-38, and Taglu G-33 wells to generate a sediment porosity curve for the subpermafrost portion of the Taglu C-42 well. The 'projected' porosities for the gas-hydrate-bearing stratigraphic units in the Taglu C-42 well averaged 34% (Table 3). The water saturations (S_w) (gas hydrate saturation (Sh) is equal to (1.0-S_w)) calculated with the Archie relation within the gas-hydrate-bearing interval of the Taglu C-42 well are very high, averaging 98% (Table 3).

SEISMIC DATA INTERPRETATION

Seismic detection of gas hydrate and free gas

In studies of deep marine gas hydrate accumulations, seismic reflection surveys are often used to identify, map, and quantify the occurrence of gas hydrate (Dillon et al., 1993). Gas hydrate has a very strong effect on acoustic seismic reflections because it is characterized by very high acoustic velocities (about 3.35 km/s, Collett, 1998a), and thus gas-hydrate-bearing sediments are characterized by high acoustic velocities. In comparison, sediments below the zone of predicted gas hydrate stability, if water saturated, have lower acoustic velocities (acoustic velocity of water is about 1.5 km/s), and if gas is trapped below the gas hydrate, the velocity is much lower even if just a few per cent of gas are present. Because of the strong acoustic impedance difference between gas-hydrate-bearing sediments and underlying free-gas-bearing sediments, the base of the gas-hydrate-

bearing zone produces a strong seismic reflection. In marine environments this strong reflector at the base of gas-hydrate-bearing sediments has become known as the bottom-simulating reflector or 'BSR'. An additional feature of a gas-hydrate-bearing sediment is caused by the abrupt acoustic velocity decrease at the bottom-simulating reflector which is caused by moving from gas-hydrate-bearing sediments above to commonly free-gas-bearing sediments below. This downward velocity decrease, known as an 'inversion', can cause an amplitude phase reversal which can be detected on seismic reflection profiles (Dillon et al., 1993). The high amplitude nature of a bottom-simulating reflector is often compared to bright spots in petroleum exploration which can be characterized by a phase shift (reversal), velocity pull-down, and strong intrinsic attenuation. It should also be noted that gas-bearing sediments, even in the absence of overlying gas hydrate, often appear as high-amplitude anomalies and can be easily identified on seismic profiles from both marine and terrestrial environments.

Until this study, bottom-simulating reflectors or other acoustic seismic anomalies associated with the occurrence of gas hydrate in onshore settings had never been reported in the literature. The lack of reported acoustic seismic anomalies associated with onshore gas hydrate accumulations is probably due to the geologically complex nature of most terrestrial gas hydrate accumulations. In general, the geology of onshore gas hydrate accumulations are relatively more complex than the geology of most marine gas hydrate accumulations. Marine gas hydrate accumulations, such as those on the Blake Ridge (eastern continental margin of North America), occur within a thick uniform stratigraphic section of mostly silt and clay (Collett, 1998a). However, terrestrial gas hydrate, such as those on the North Slope of Alaska (Collett, 1993) or in the Mackenzie River Delta (Collett et al., 1999), occur within complexly interbedded sandstone and shale sequences, with the gas hydrate concentrated in the high-porosity reservoir-quality sandstone units. Therefore, a reflection seismic profile across a known terrestrial gas hydrate accumulation will not exhibit a classical marine-type bottom-simulating reflector. Instead, the interbedded gas-hydrate-bearing sandstone layers and non-gas-hydrate-bearing shale layers appear as a series of interbedded high- and low-amplitude reflectors and in some cases, at the base of the gas hydrate stability zone along a given seismic reflector, a distinct phase reversal may be detected.

General results

Synthetic seismograms constructed from acoustic transit-time and electrical resistivity logs from the 11 wells examined in this study were used to correlate the surface seismic data with the well information in the Ivik–Mallik–Taglu area (Fig. 8). We were then able to interpret regional geology and more precisely determine the occurrence of gas hydrate and associated free gas in the study area. Synthetic seismograms can be used to accurately convert known well-log depths for a particular horizon to a measured acoustic seismic depth. To further characterize the acoustic velocity structure of the near-surface sediments in the Ivik–Mallik–Taglu study area, we have also generated acoustic transit-time depth profiles (Fig. 9) as measured directly from the acoustic log data in nine of the wells examined in this study. The interpolated seismic time-depth plots in Figure 9 show a relatively consistent velocity structure with depth in the upper 1 km of sediment in the Ivik–Mallik–Taglu study area. The only notable exception is the relatively slow velocity model predicted for the nearshore Mallik P-59 well in which the velocity of the permafrost interval is probably affected by low ice concentrations.

For each of the wells examined in this study we have obtained the depths to the contacts between each of the major sequence boundaries (Iperk–Mackenzie Bay sequence boundary, Mackenzie Bay–Kugmallit sequence boundary, and the Kugmallit–Richards sequence boundary) within the upper 3000 m of the stratigraphic section on Richards Island (J. Dixon, pers. comm., 1999) (Table 1). We have used the interpreted seismic time-depth plot in Figure 9 and the well-log-derived synthetic seismograms to interpret the depth of the major sequence boundaries on the available seismic profiles from the Ivik–Mallik–Taglu area (Table 2, Fig. 2, 7). We have also used the available seismic data to map the numerous large-scale faults and structures in the Ivik–Mallik–Taglu area.

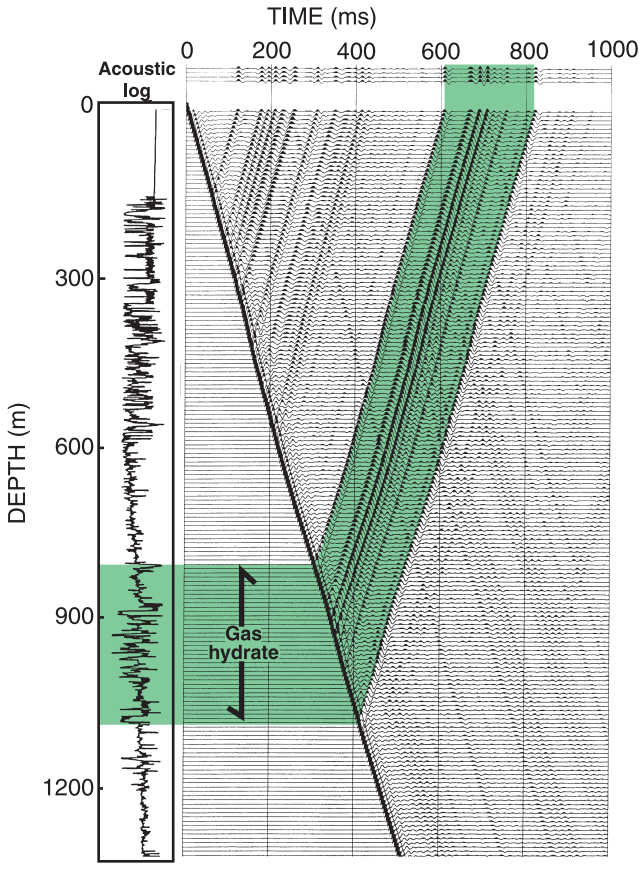

Figure 8. *Example of a synthetic seismogram generated from the downhole well-log data in the Mallik L-38 well. Noted on this diagram is the depth of the well-log-inferred gas-hydrate-bearing interval (810.1–1102.3 m) in the Mallik L-38 well.*

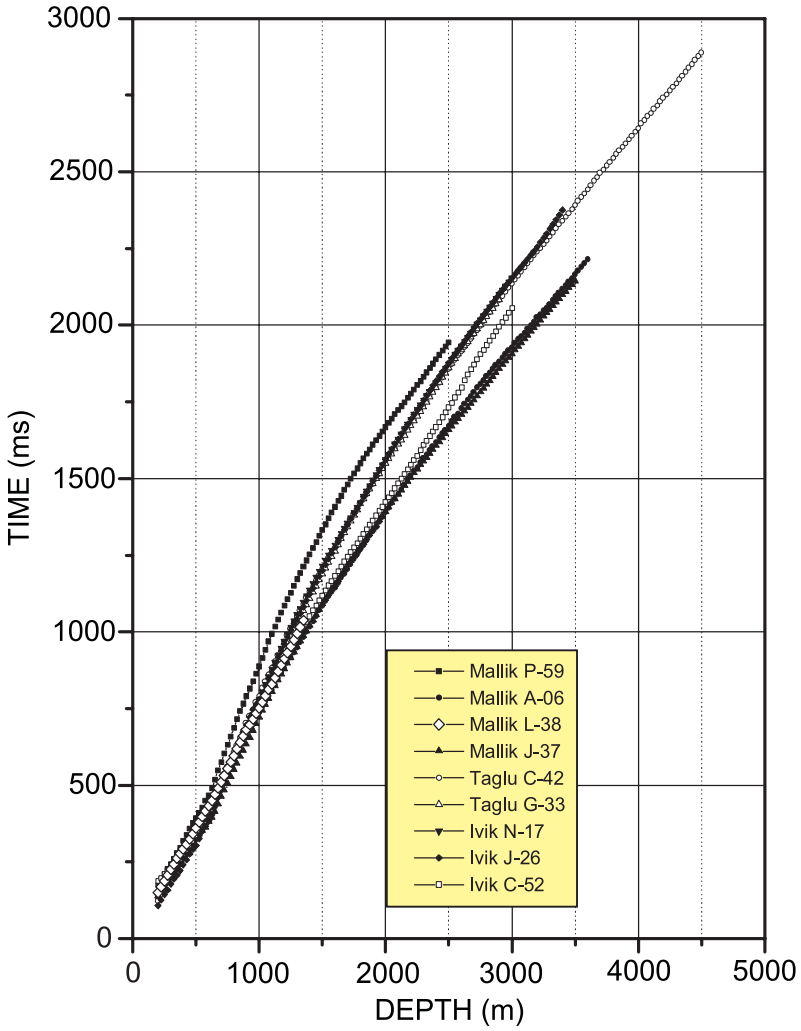

Figure 9.

Plot of two-way seismic travel-time versus depth calculated from available downhole acoustic transit-time and electrical resistivity well-log data from nine of the wells examined in this study.

We have thoroughly analyzed all of the 13 reflection seismic profiles (Table 2, Fig. 2) provided by Imperial Oil Limited. In Figure 7 we have shown six representative seismic profiles from the Ivik–Mallik–Taglu area. As a condition of the seismic data release from Imperial Oil Limited, we are permitted to show only the upper two seconds of seismic data and all of the shot-point information had to be removed from the published seismic profiles.

The sequence boundaries depicted on the seismic profiles in Figure 7 have been shown mainly for reference purposes. As shown on Figure 7, the entire Iperk Sequence contains very few seismically visible structures, with the exception of local sedimentary slumping features. Beneath the Iperk Sequence strata, the Mackenzie Bay and Kugmallit sequences are disrupted by numerous large-scale listric faults, with predominantly down-to-basin throws. The initial development of these faults was probably related to the progradation of the Kugmallit Sequence delta across older, unstable shelf margins. Regionally, the throw on these large-scale listric faults often exceed 100–500 m. Closer examination of the available seismic data also reveals numerous small-scale faults over the crest of the major anticlinal features, which are characterized by small offset faults ranging from 20 m to 50 m. The other most prominent seismic feature of the Ivik–Mallik–Taglu area are two large southeast-trending anticlines in the area of the Mallik and Ivik C-52 wells (Fig. 7). The Ivik–Mallik–Taglu seismic data also reveals several more subtle anticlinal structures in the area of Taglu (near Taglu C-42 and Taglu G-33) and to the north near the Ivik J-26 and Ivik N-17 wells. For discussion purposes we have named the large-scale anticlinal features in the Mallik area and at the site of the Ivik C-52 well the Mallik and Ivik C-52 anticlines, respectively. We have also named the more subtle anticlinal features in the Taglu area and at the site of the Ivik J-26 and Ivik N-17 wells the Taglu and North Ivik anticlines, respectively.

The primary goal of the seismic analysis portion of this study was to directly detect and map the gas hydrate and associated free-gas accumulations in the Ivik–Mallik–Taglu area using the available seismic data. The seismic interpretation of gas hydrate and free gas in the Ivik–Mallik–Taglu study area relied on the integration of information on the depth of the pressure-temperature predicted base of the gas hydrate stability zone with the acoustic properties (i.e. amplitude anomalies, phase reversals, etc.) of the sedimentary section imaged on the available seismic profiles. On each of the

seismic lines in Figure 7 we have shown the base of the gas hydrate stability zone. This phase boundary between gas hydrate and free gas has been estimated from temperature profiles in area wells and directly interpreted by the appearance of amplitude phase reversals and other amplitude anomalies at the predicted base of gas hydrate. We have also attempted to identify amplitude anomalies (correlated with well-log data interpretations) associated with the occurrence of free gas and gas hydrate.

At the site of the known gas hydrate accumulations in the Mallik wells, the available seismic profiles reveal numerous high-amplitude reflectors (highlighted *in* Fig. 7) along the crest of the Mallik anticline extending from a seismic time of about 0.6 s to below 1.0 s. This relatively thick package of high-amplitude reflectors are probably the gas-hydrate-bearing and free-gas-bearing units encountered in the Mallik wells. Of particular interest is the apparent seismic phase reversal associated the base of the gas hydrate stability zone beneath the crest of the Mallik anticline as shown on seismic profile 85251 (Fig. 7a). Further review of the seismic profiles in Figure 7, also reveal that the well-log-inferred gas hydrate accumulations in the Taglu and Ivik areas are also characterized by relatively thick packages of high-amplitude reflectors associated with the Taglu, Ivik C-52, and North Ivik anticlines.

Our assessment of the regional seismic profiles depicted in Figure 7 has revealed the occurrence of significant gas hydrate-related free-gas accumulations along the crest and flanks of both the Mallik and Ivik C-52 anticlines. The apparent high-amplitude nature of the seismic reflectors along the flanks of these structures has been used as the primary evidence for the occurrence of free gas associated with the overlying gas hydrate accumulations. Of interest, however, is the apparent lack of significant free-gas immediately below the crest of the Mallik and Ivik C-52 structures. In general, the structural geometry and the interbedded nature of the sedimentary section associated with these structures appear to concentrate free gas, which likely migrated from depth (Lorenson et al., 1999), in the flanks of these major regional features. It also appears that both smaller local and large-scale regional faults control the migration and accumulation of hydrocarbon gas on Richards Island.

Specific results

To examine the structural features and gas hydrate accumulations in the Ivik–Mallik–Taglu area of the Richards Island we have considered six adjacent seismic profiles: 85251, 85987, 86055, 85988, 85984, and 84942. Interpreted portions of these seismic profiles and their locations are shown in Figure 7.

Seismic profile 85251

Seismic profile 85251 runs from the southwest corner of the study area to the northeast and crosses both the Taglu and Mallik anticlines. The most prominent feature of this profile is the Mallik anticline which is bounded to the southwest by a relatively large-scale normal fault (downthrown into the basin). We have shown the predicted base of the methane hydrate stability zone to cross the Mallik anticline at a time depth of about 0.9 s, which coincides with the occurrence of a distinct phase reversal at the crest of the Mallik structure. We have interpreted that the crest of the Mallik anticline contains a thick sequence of gas-hydrate-bearing and free-gas-bearing sediments. Based on the analysis of well-log and seismic data we have also inferred the occurrence of gas hydrate and associated free-gas accumulations along the northern flank of the Taglu anticline.

Seismic profile 85987

Seismic profile 85987 also crosses the Mallik anticline and runs to the north where it crosses the down-dip plunge of the Ivik C-52 anticline. The Mallik anticline is again one of the most prominent features on line 85987, however, the crest of the structure appears to be cut by a number of high-angle normal faults that were not visible on profile 85251. The apparent phase reversal on profile 85251 at the predicted base of the methane hydrate stability zone is not as prominent on profile 85987. The base of the gas hydrate stability zone on profile 85987 is marked by several subtle phase reversals on the northern flank of the Mallik anticline. As imaged on profile 85987, the Ivik C-52 anticline appears to be a composite of two smaller anticlinal structures, separated by relatively large normal faults extending well into the upper part of the stratigraphic section. Based on the analysis of both well-log and seismic data we have also inferred the occurrence of gas hydrate and associated free-gas accumulations along the crest of the Ivik C-52 anticline.

Seismic profile 86055

Seismic profile 86055 runs from southwest to northeast across the study area and crosses both the Mallik and Ivik C-52 anticlines. The appearance of seismic profile 86055 is similar to the general appearance of seismic profile 85987. Relative to profile 85987, the Mallik anticline on profile 86055 is apparently more tightly folded and the top of the Kugmallit Sequence over the Mallik anticline is slightly shallower, which conforms to the apparent plunge of the Mallik anticline to the northwest. The base of the gas hydrate stability zone on profile 86055 appears to be marked by the termination of several free-gas-associated seismic reflectors at the base of the seismically inferred gas hydrate accumulation near the crest of the Mallik anticline. The Ivik C-52 anticline appears as a single tightly folded anticline with the northern flank of the structure forming a monocline. On the southern flank of the Ivik C-52 anticline, the base of the gas hydrate stability zone on profile 86055 is marked by distinct phase reversal along a steeply dipping seismic reflector. The combined analysis of seismic profile 86055 with available well-log data, also infers the occurrence of gas hydrate and associated free-gas accumulations along the crest and flanks of both the Mallik and Ivik C-52 anticlines.

Seismic profile 85988

Seismic profile 85988 is a relatively short line running nearly north-south through the centre of the study area. The Mallik anticline is again the most prominent feature on profile 85988; however, in comparison to the other profiles that cross this structure, the Mallik anticline as imaged on profile 85988 is more broadly folded with relatively gentle dips along the south and north flanks of the structure. At the northern end of the seismic profile 85988, the southern flank of the Ivik C-52 anticline is also imaged. The predicted base of the methane hydrate stability zone crosses the Mallik anticline on line 85988 at a time depth of about 0.85 s, and is marked by several subtle seismic phase reversals along the southern flank of the structure. We have again inferred the occurrence of gas hydrate and free gas in the Mallik anticline and along the southern flank of the Ivik C-52 structure.

Seismic profile 85984

Seismic profile 85984 crosses the Ivik C-52 anticline and runs from southwest to northeast across the study area. On profile 85984, the Ivik C-52 structure appears as a very prominent symmetrically folded anticline, with the crest of the structure extending to the base of the Iperk Sequence. The predicted base of the methane hydrate stability zone crosses the Ivik C-52 anticline at a time depth of about 1.0 s, which coincides with several subtle seismic phase reversals and the termination of several free-gas-associated high-amplitude reflectors along both the southern and northern flanks of the Ivik C-52 structure. Our interpretation of profile 85984 combined with the analysis of the acoustic and electrical resistivity log data from the Ivik C-52 well (Table 3) also infers the occurrence of gas hydrate and associated free-gas accumulations along the crest and flanks of the Ivik C-52 anticline.

Seismic profile 84942

Seismic profile 84942, in the northeast corner of the study area, cuts directly through the location of the Ivik J-26 well which has been the focus of gas hydrate studies in the past (Bily and Dick, 1974). Seismic profile 84942 reveals the gently asymmetrically folded nature of the North Ivik anticline. The predicted base of the methane hydrate stability zone on profile 84942 is marked by the down-dip termination of several gas hydrate-associated high-amplitude reflectors near the crest of the North Ivik structure. Based mainly on the occurrence of well-log-inferred gas hydrate in the Ivik J-26 well, we have interpreted the high-amplitude reflectors near the top of the North Ivik anticline to be caused by gas hydrate restricted to the crest of the structure.

INTEGRATED SEISMIC- AND LOG-DATA INTERPRETATION

As previously indicated in this report, the integration of information from conventional open-hole well-log surveys in 11 industry wells and over 240 km of industry-acquired reflection seismic data has allowed the identification and analysis of four distinct gas hydrate accumulations on Richards Island, 1) Mallik, 2) Ivik C-52, 3) North Ivik, and 4) Taglu gas hydrate accumulations. The map in Figure 10 depicts the seismically inferred distribution of the four gas hydrate accumulations on Richards Island. The boundaries of the four gas hydrate accumulations shown in Figure 10 depict the location of the outermost edge (hydrate-water or hydrate-gas contact) of each gas hydrate accumulation as imaged with the available seismic data (Fig. 7). Well-log data from the 11 wells examined in this study have also been used to assess the distribution and concentration of gas hydrate in each of the seismic and well-log-inferred gas hydrate accumulations. The following section of this report includes descriptions of the four well-log- and seismically inferred gas hydrate accumulations on Richards Island and estimates of the volume of gas trapped as gas hydrate in each of the four accumulations.

Before proceeding with the description of the Richards Island gas hydrate accumulations, it is necessary to review the procedures used to calculate the volume of gas within each of the delineated gas hydrate accumulations. The volume of gas that may be contained in a gas hydrate accumulation depends on the following five 'reservoir' parameters (Collett, 1993): 1) areal extent of the gas hydrate occurrence, 2) reservoir thickness, 3) sediment porosity, 4) degree of gas hydrate saturation, and 5) the hydrate gas yield volumetric parameter which defines how much free gas (at Standard Temperature and Pressure; STP) is stored within a gas hydrate. For this 'resource' assessment, we have defined the thickness of the gas-hydrate-bearing sedimentary section as the total thickness of the log-inferred gas-hydrate-bearing section in each of the nine wells thought to have penetrated gas hydrate (Table 3). The density-log-derived porosities from each of the wells examined were used to calculate the required sediment porosities in the wells thought to have encountered gas hydrate (Table 3). Gas hydrate saturations (Sh) in the gas-hydrate-bearing units of the nine wells thought to have penetrated gas hydrate were calculated from the standard Archie relation (Table 3). In this assessment we have assumed a hydrate number of 6.325 (90% gas-filled clathrate) which corresponds to a gas yield of 164 m^3 of methane (at STP) for every cubic metre of gas hydrate. Based on these assumptions we have calculated the volume of gas trapped as gas hydrate within the one square kilometre area surrounding each of the nine wells believed to have encountered gas hydrate (Table 3). To calculate the total volume of gas within each of the gas hydrate accumulations depicted on the map in Figure 10, the well-log-calculated 'per-well hydrate gas yields' (volume of gas trapped as gas hydrate within the one square kilometre area surrounding each well) for each well listed in Table 3 were used to systematically assess variations in gas hydrate content (saturations) within each of the delineated accumulations (discussed in more detail later in this section). Because of incomplete well-log coverage, no attempt has been made to calculate the volume of free gas trapped below the gas hydrate accumulations on Richards Island.

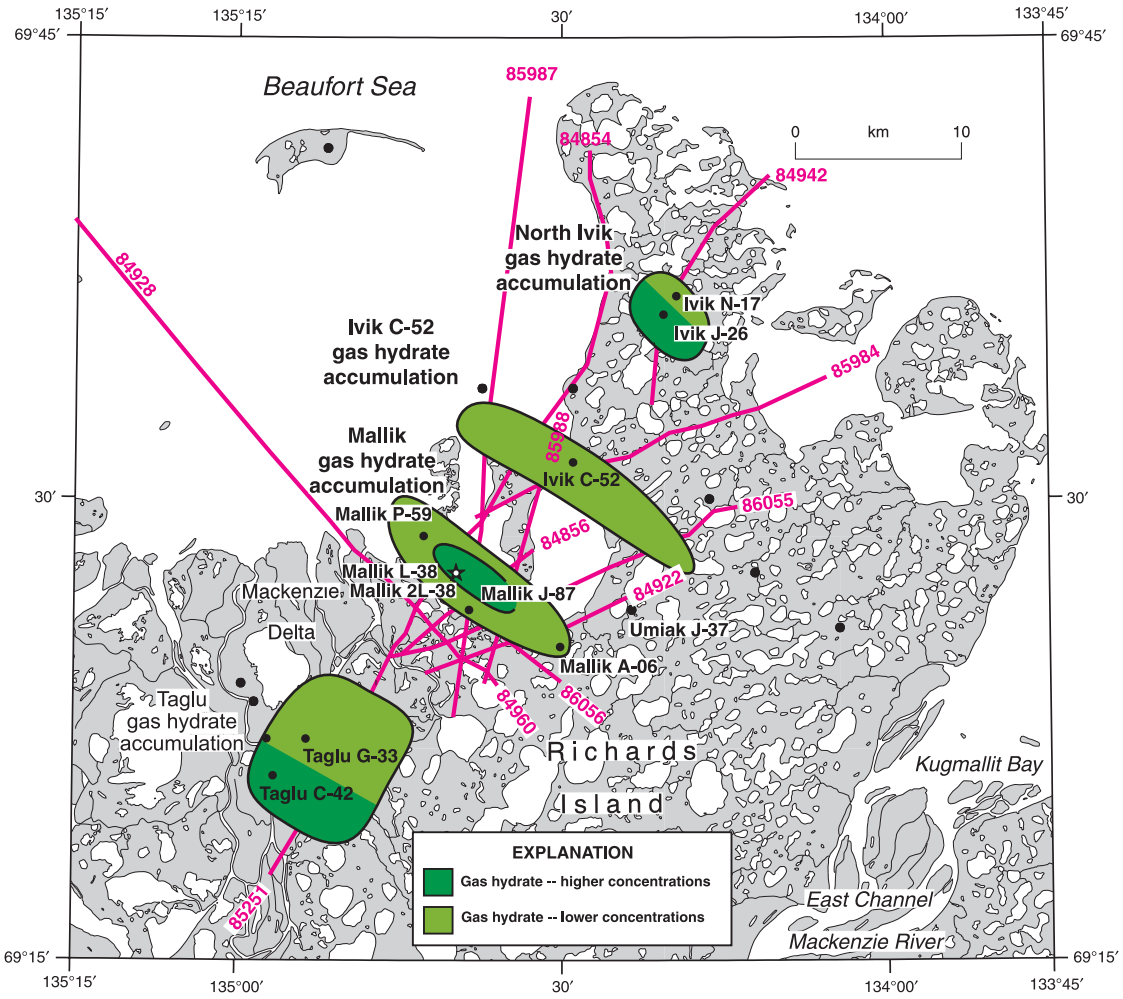

Figure 10. *Map showing the four seismic and well-log-inferred gas hydrate accumulations on Richards Island in the outer Mackenzie Delta. The portions of the delineated gas hydrate accumulations in darker shades of green denote areas of relatively higher gas hydrate concentrations.*

Mallik gas hydrate accumulation

As interpreted from the seismic profiles in Figure 7 and as depicted in Figure 10, gas hydrate deposits are inferred and known to occur along the crest of the Mallik anticline. The Mallik gas hydrate accumulation appears to be laterally continuous and is estimated to cover an area of about 51 km^2 (Table 4). However, analysis of downhole log data from the Mallik L-38, 2L-38, P-59, and A-06 wells reveal highly variable gas hydrate saturations and 'per-well hydrate gas yields' throughout the Mallik accumulation. As shown in Table 3, the 'per-well hydrate gas yield' for the Mallik wells range from 1427x10^6 m^3/km^2 to 4902x10^6 m^3/km^2 of gas. Seismic mapping and the analysis of the Mallik L-38 and 2L-38 downhole well-log data revealed that the gas hydrate deposits are more highly concentrated within the uppermost crest of the Mallik anticline (Fig. 10). Therefore, each of the 'per-well hydrate gas yields' calculated for the four wells that penetrated the Mallik gas hydrate accumulation were used as

Table 4. List of the four seismic- and well-log-inferred gas hydrate accumulations on Richards Island in the outer Mackenzie Delta. Also listed is the calculated volume of gas within the delineated gas hydrate accumulations.

Gas hydrate accumulation	Area of gas hydrate accumulation (km^2)	Volume of gas within hydrate per square km (x 10^6 m^3)	Total volume of gas within the hydrates of each gas hydrate accumulation (x 10^6 m^3)
Mallik	10.27 41.08	4835 1469	49 656 60 347 Total 110 003
Ivik C-52	46.61	921	42 928
North Ivik	15.01 9.48	1187 531	17 817 5034 Total 22 851
Taglu	26.07 38.71	351 58	9151 2245 Total 11 396

input in a statistical mapping computer program to calculate the total volume of gas trapped as gas hydrate in the Mallik anticline. This systematic resource appraisal determined that the Mallik gas hydrate accumulation contains approximately 110 003x10^6 m^3 of gas in hydrate form (Table 4).

Ivik C-52 gas hydrate accumulation

The seismic-and well-log-inferred Ivik C-52 gas hydrate accumulation, as depicted in Figure 10, is also restricted to the crest of a major northwest-trending anticlinal structure. The Ivik C-52 gas hydrate accumulation is estimated to cover an area of more than 46 km^2 (Table 4). Only one well has penetrated the Ivik C-52 gas hydrate accumulation (i.e. Ivik C-52), in which the 'per-well hydrate gas yield' factor was calculated at 921x10^6 m^3/km^2 of gas. Since the Ivik C-52 anticline was penetrated by only one well, the volume of gas within the Ivik C-52 gas hydrate accumulation was determined by simply multiplying the seismically inferred area of the gas hydrate accumulation (46.6 km^2) by the 'per-well hydrate gas yield' factor, which yields a total gas volume for the Ivik C-52 gas hydrate accumulation of 42 928x10^6 m^3 of gas (Table 4).

North Ivik gas hydrate accumulation

The North Ivik gas hydrate accumulation appears to be limited to a series of relatively thin sandstone units at the crest of the North Ivik anticline. Based on the available seismic data, we were unable to determine the lateral extent of the North Ivik gas hydrate accumulation. In comparison to the Ivik N-17 well, the concentration of the well-log-inferred gas hydrate in the Ivik J-26 well is relatively high (Table 3). Due to the variable nature of the gas hydrate concentrations in the North Ivik accumulation we used a statistical mapping computer program and the 'per-well hydrate gas yield' factors from the Ivik N-17 and J-26 wells to calculate the total volume of gas trapped as gas hydrate in the North Ivik anticline. This systematic gas hydrate resource appraisal of the North Ivik gas hydrate accumulation yielded a calculated gas volume of 22 851x10^6 m^3 of gas trapped as hydrate in the North Ivik anticline (Table 4).

Taglu gas hydrate accumulation

Seismic data from the Taglu area along with downhole log data from the Taglu G-33 and C-42 wells reveal that the Taglu gas hydrate accumulation is restricted to a series of relatively thin sandstone units along the northern flank of the Taglu anticline. However, due to the limited number of seismic lines, we were unable to determine the lateral extent of the Taglu gas hydrate accumulation. Well-log-calculated gas hydrate saturations in the Taglu gas hydrate accumulation are variable and generally very low (Table 3). Due to the variable nature of gas hydrate saturations in the Taglu gas hydrate accumulation we used a statistical mapping computer program and the 'per-well hydrate gas yield' factors for the Taglu G-33 and C-42 wells to calculate the total volume of gas trapped as gas hydrate in the Taglu anticline. This systematic gas hydrate resource assessment yielded a calculated gas volume of 11 396x10^6 m^3 of gas trapped as hydrate in the Taglu anticline (Table 4).

SUMMARY

The primary objective of this study was to assess the distribution and size of the gas hydrate accumulations on Richards Island in the outer Mackenzie Delta. Gas hydrate has been conclusively identified in the Mallik 2L-38 gas hydrate research well and is inferred to occur in an additional eight industry exploratory wells on Richards Island. The integration of industry-acquired seismic reflection data with the available open-hole log data from the 11 wells examined in this study documents the occurrence of four distinct gas hydrate accumulations on Richards Island, 1) Mallik, 2) Ivik C-52, 3) North Ivik, and 4) Taglu gas hydrate accumulations. The total volume of gas (in place) trapped as gas hydrate in these four gas hydrate accumulations is estimated at 187 178x10^6 m^3.

For the most part, the seismic- and well-log-inferred gas hydrate accumulations on Richards Island are restricted to the crest of large anticlines where the base of the gas hydrate stability zone intercepts the crest of these structural features. The distribution of these four distinct gas hydrate accumulations appear to be controlled in part by the presence of anticlines that may have acted as conventional hydrocarbon traps. Considering that the gas hydrate accumulations on Richards Island are restricted to conventional hydrocarbon traps and the gas associated with the sampled gas hydrate accumulations in the Mallik 2L-38 well may have migrated from a more deeply buried thermogenic source, it is likely that some portion of the Richards Island gas hydrate accumulations originated from migrated thermogenic gas that was first concentrated in shallow traps as conventional free-gas fields that were later converted to gas hydrate fields in response to climate cooling or changes in surface conditions. The occurrence of gas hydrate in conventional hydrocarbon traps provides us with an exploration model and play concept that may be used to predict the occurrence of gas hydrate in unexplored Arctic regions.

REFERENCES

Allen, D.M., Michel, F.A. and Judge, A.S.
1988: The permafrost regime in the Mackenzie Delta, Beaufort Sea region, Northwest Territories and its significance to the reconstruction of the paleoclimatic history; Journal of Quaternary Science, v. 3, p. 3–13.

Archie, G.E.
1942: The electrical resistivity log as an aid in determining some reservoir characteristics; Journal of Petroleum Technology, v. 5, p. 1–8.

Bily, C. and Dick, J.W.L.
1974: Natural occurring gas hydrates in the Mackenzie Delta, Northwest Territories; Bulletin of Canadian Petroleum Geology, v. 22, p. 340–352.

Collett, T.S.
1993: Natural gas hydrates of the Prudhoe Bay and Kuparuk River area, North Slope, Alaska; American Association of Petroleum Geologists Bulletin, v. 77, no. 5, p. 793–812.

Collett, T.S. (cont.)
1998a: Well log evaluation of gas hydrate saturations; *in* Transactions of the Society of Professional Well Log Analysts, Thirty-ninth Annual Logging Symposium, May 26–29, 1998, Keystone, Colorado, Paper MM, Society of Professional Well Log Analysts.
1998b: Well log characterization of sediment porosities in gas-hydrate-bearing reservoirs; *in* Proceedings of the 1998 Annual Technical Conference and Exhibition of the Society of Petroleum Engineers, September 27–30, 1998, New Orleans, Louisiana, 12 p.

Collett, T.S. and Dallimore, S.R.
1998: Quantitative assessment of gas hydrates in the Mallik L-38 well, Mackenzie Delta, N.W.T., Canada; *in* Proceedings of the Seventh International Conference on Permafrost, June 23–27, 1998, Yellowknife, N.W.T., Canada, Collection Nordicana, Université Laval, p. 189–194.

Collett, T.S., Lewis, R., Dallimore, S.R., Lee, M.W., Mroz, T.H., and Uchida, T.
1999: Detailed evaluation of gas hydrate reservoir properties using JAPEX/JNOC/GSC Mallik 2L-38 gas hydrate research well downhole well-log displays; *in* Scientific Results from JAPEX/JNOC/GSC Mallik 2L-38 Gas Hydrate Research Well, Mackenzie Delta, Northwest Territories, Canada, (ed.) S.R. Dallimore, T. Uchida, and T.S. Collett; Geological Survey of Canada, Bulletin 544.

Cranston, R.E.
1999: Pore-water geochemistry, JAPEX/JNOC/GSC Mallik 2L-38 gas hydrate research well; *in* Scientific Results from JAPEX/JNOC/GSC Mallik 2L-38 Gas Hydrate Research Well, Mackenzie Delta, Northwest Territories, Canada, (ed.) S.R. Dallimore, T. Uchida, and T.S. Collett; Geological Survey of Canada, Bulletin 544.

Dallimore, S.R. and Collett, T.S.
1995: Intrapermafrost gas hydrates from a deep core hole in the Mackenzie Delta, Northwest Territories, Canada; Geology, v. 23, p. 527–530.
1998: Gas hydrates associated with deep permafrost in the Mackenzie Delta, N.W.T., Canada: regional overview; *in* Proceedings of the Seventh International Conference on Permafrost, June 23–27, 1998, Yellowknife, N.W.T., Canada, Collection Nordicana, Université Laval, p. 201–206.
1999: Regional gas hydrate occurrences, permafrost conditions, and Cenozoic geology, Mackenzie Delta area; *in* Scientific Results from JAPEX/JNOC/GSC Mallik 2L-38 Gas Hydrate Research Well, Mackenzie Delta, Northwest Territories, Canada, (ed.) S.R. Dallimore, T. Uchida, and T.S. Collett; Geological Survey of Canada, Bulletin 544.

Dillon, W.P., Lee, M.W., Fehlhaber, K., and Coleman, D.F.
1993: Gas hydrates on the Atlantic continental margin of the United States—controls on concentration; *in* The Future of Energy Gases, (ed.) D.G. Howell; United States Geological Survey, Professional Paper 1570, p. 313–330.

Dixon, J., Dietrich, J.R., and McNeil, D.H.
1992: Upper Cretaceous to Pleistocene Sequence Stratigraphy of the Beaufort-Mackenzie and Banks Island Areas, Northwest Canada; Geological Survey of Canada, Bulletin 407, p. 1–90.

Dixon, J.D., Morrell, G.R., Dietrich, J.R., Taylor, G.C., Procter, R.M., Conn, R.F., Dallaire, S.M., and Christie, J.A.
1994: Petroleum resources of the Mackenzie Delta and Beaufort Sea; Geological Survey of Canada Bulletin, v. 474, p. 1–52.

Jenner, K.A., Dallimore, S.R., Clark, I.D., Paré, D., and Medioli, B.E.
1999: Sedimentology of gas hydrate host strata from the JAPEX/JNOC/GSC Mallik 2L-38 gas hydrate research well; *in* Scientific Results from JAPEX/JNOC/GSC Mallik 2L-38 Gas Hydrate Research Well, Mackenzie Delta, Northwest Territories, Canada, (ed.) S.R. Dallimore, T. Uchida, and T.S. Collett; Geological Survey of Canada, Bulletin 544.

Judge, A.S.
1986: Permafrost distribution and the Quaternary history of the Mackenzie-Beaufort region: a geothermal perspective; *in* Correlation of Quaternary Deposits and Events around the Margin of the Beaufort Sea (ed.) J.A. Heginbottom and J.S. Vincent; Geological Survey of Canada, Open File 1237, p. 41–45.

Judge, A.S. and Majorowicz, J.A.
1992: Geothermal conditions for gas hydrate stability in the Beaufort-Mackenzie area: the global change aspect; Global and Planetary Change, v. 98, p. 251–263.

Lee, M.W. and Agena, W.F.
1998: Seismic processing for gas hydrate research drill site in the Mackenzie Delta, Canada; United States Geological Survey, Open File Report 593, 14 p.

Lorenson, T.D., Whiticar, M., Waseda, A., Dallimore, S.R., and Collett, T.S.
1999: Gas composition and isotopic geochemistry of cuttings, core, and gas hydrate from the JAPEX/JNOC/GSC Mallik 2L-38 gas hydrate research well; *in* Scientific Results from JAPEX/JNOC/GSC Mallik 2L-38 Gas Hydrate Research Well, Mackenzie Delta, Northwest Territories, Canada, (ed.) S.R. Dallimore, T. Uchida, and T.S. Collett; Geological Survey of Canada, Bulletin 544.

Majorowicz, J. and Smith, S.
1999: Review of ground temperatures in the Mallik field area: a constraint to the methane hydrate stability; *in* Scientific Results from JAPEX/JNOC/GSC Mallik 2L-38 Gas Hydrate Research Well, Mackenzie Delta, Northwest Territories, Canada, (ed.) S.R. Dallimore, T. Uchida, and T.S. Collett; Geological Survey of Canada, Bulletin 544.

Pearson, C.F., Halleck, P.M., McGuire, P.L., Hermes, R., and Mathews, M.
1983: Natural gas hydrate deposit: a review of in situ properties; Journal of Physical Chemistry, v. 87, p. 4180–4185.

Procter, R.M., Taylor, G.C., and Wade, J.A.
1984: Oil and natural gas resources of Canada 1983; Geological Survey of Canada, Paper 83-31, p. 1–59.

Sloan, D.
1990: Clathrate Hydrates of Natural Gases; Marcel Dekker, New York, New York, 641 p.

Smith, S.L. and Judge, A.S.
1993: Gas hydrate database for Canadian Arctic and selected east coast wells; Geological Survey of Canada, Open File 2746, p. 1–7.

Snowdon, L.R. and Powell, T.G.
1982: Immature oil and condensate—modification of hydrocarbon generation model for terrestrial organic matter; American Association of Petroleum Geologists Bulletin, v. 66, p. 775–788.

Natural Resources Canada Ressources naturelles Canada

GEOLOGICAL SURVEY OF CANADA COMMISSION GÉOLOGIQUE DU CANADA

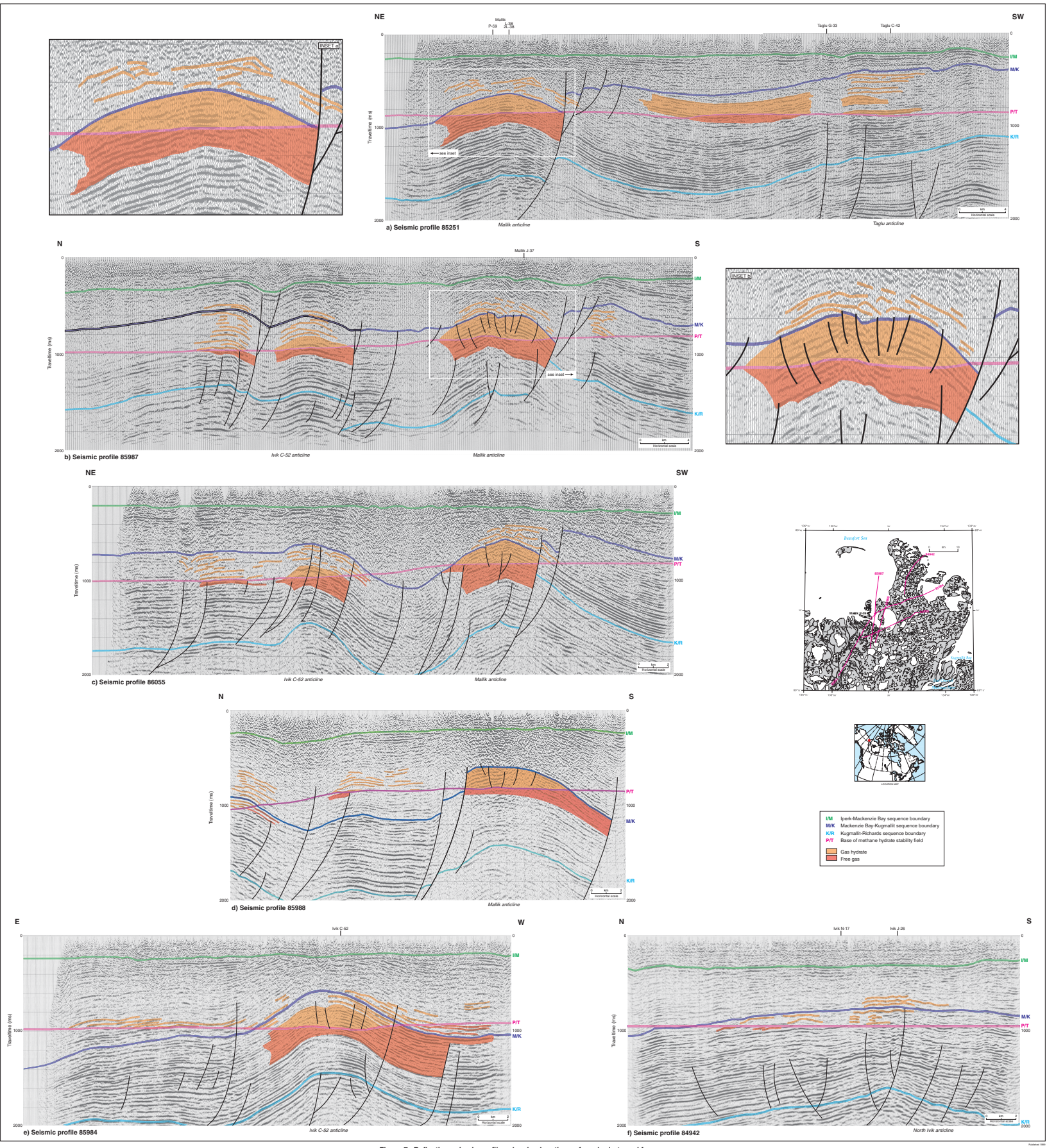

Figure 7. Reflection seismic profiles showing locations of gas hydrate and free-gas accumulations, major sequence boundaries, large-scale faults, and structures in the Ivik–Mallik–Taglu area.